

Table 2. Percentage of differentiated marker-positive cells in each differentiating condition.

Cells	Tg ⁺	β-III-tub ⁺	Oil-red-O ⁺
PT-0808	96.8	67.1	87.0
PT-0902	93.9	55.0	48.6

% of positive cells.

doi:10.1371/journal.pone.0019354.t002

of the cells by analyzing expressions of STRO-1 and two intermediate filaments, cytokeratin-18 and vimentin. In our system, there were only two types of attached cells in terms of expression pattern of the above-mentioned markers after initial plating: cytokeratin-18/vimentin double-positive cells and STRO-1/vimentin double-positive cells. Thyroid follicular cells coexpress cytokeratin-18 and vimentin, which is consistent with earlier studies [18,19,20]. Cytokeratin-18/vimentin-positive cells may also contain a small number of endothelial cells since several papers demonstrated expression of cytokeratin in microvascular endothelial cells in different tissues [21,22,23,24,25]. STRO-1/vimentin-positive cells are perhaps composed of premature mesenchymal cells. The SAGM-grown cells were propagated from thyroid follicular cells (or at least thyroid-committed cells) because: (1) the SAGM-grown cells were negative for STRO-1; (2) the cells lost cytokeratin-18 expression during expansion; (3) STRO-1-positive cells did not proliferate; (4) *TG* mRNA expression was also decreased during proliferation but still detectable after 3–5 weeks; (5) the SAGM-grown cells were propagated from sorted TPO^{hi} cells.

Although both cytokeratin-18 and vimentin expressions were observed even in undifferentiated thyroid cancer cell lines, the cytokeratin-18 expression was lost in the SAGM-grown cells. All of thyroid-specific gene expressions were not observed in the cells. Moreover, the SAGM-grown cells displayed high plasticity: multilineage differentiation potential into thyrocytes, neuronal cells and adipocytes. These results suggest that we have successfully dedifferentiated/converted thyroid follicular cells into multilineage progenitor cells. However, re-differentiation effects (expression level of thyroid-specific genes) were modest compared to PT. We are currently seeking the better method enabling more efficient differentiation. In addition, these cells do not have unlimited proliferative capacity: the cells will stop growing until 3–4 months, due to cellular senescence.

Conversion of differentiated cells into multipotent progenitor or different lineage has been reported by several groups. Adult hepatocytes were converted into insulin-producing cells by transgenes, *Pdx-1* and *Ngn-3* [26]; retinal pigment epithelium into retinal neurons by *Sox-2* [27]; and interfollicular epidermal basal keratinocytes into the cells capable of differentiating into neuronal cells by *Oct-4* [28]. The aforementioned studies used exogenous transgenes, some of which are key transcription factors for generating iPS cells. To our knowledge, there is only one report describing conversion from differentiated cells into multilineage progenitor cells without any gene delivery. Adult intestinal epithelial cells were dedifferentiated into nestin-positive cells that have multilineage differentiation capacity into neuronal, pancreatic and hepatic lineages [29]. The authors cultured intestinal epithelial cells on mouse embryonic fibroblasts (feeder layer) in medium supplemented with leukemia inhibitory factor, EGF and bFGF. For generating iPS cells, two key transcription factors Klf-4 and Sox-2 could be replaced by chemical compounds [30,31].

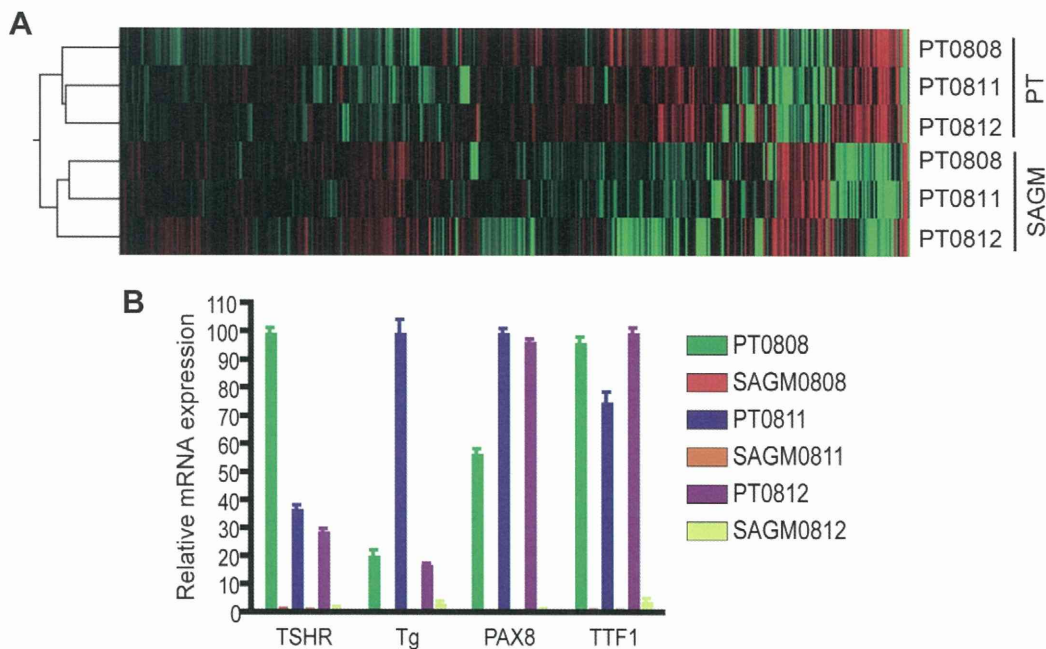


Figure 4. Microarray analysis of PT and corresponding SAGM-grown cells. A, The tree view of hierarchical clustering. PT: total RNA was extracted from PT on the next day of plating. SAGM: the SAGM-grown cells were expanded for two weeks and subcultured. On the next day, total RNA was extracted. The total RNAs were subjected to Affymetrix GeneChip Human Genome U133 Plus 2.0 microarray analysis service. Hierarchical clustering (by Manhattan distance) was performed using probes with “present call” only. Red columns represent higher expression, and green indicate lower expression. B, Confirmation of microarray data. Total RNA was subjected to qRT-PCR for indicated genes. Each bar indicates the mean and SD of the data collected in triplicate.
doi:10.1371/journal.pone.0019354.g004

Table 3. Fold-change of interested genes (SAGM cells/PT).

Gene	Probe	PT0808			PT0811			PT0812		
		PT-flag	SAGM-flag	fold	PT-flag	SAGM-flag	fold	PT-flag	SAGM-flag	fold
ABCG2	209735_at	A	A		A	A		A	A	
Oct4	208286_x_at	A	A		A	A		A	A	
CD133	204304_s_at	P	A	0.00	P	A	0.03	P	A	0.04
TG	203673_at	P	A	0.05	P	A	0.00	P	A	0.19
TSHR	210055_at	P	A	0.04	P	A	0.16	P	A	0.04
	215442_s_at	P	P	0.06	P	A	0.25	P	P	0.20
	215443_at	P	P	0.06	P	A	0.02	P	A	0.05
	237349_at	A	A		A	A		A	A	
PAX8	121_at	P	P	0.06	P	P	0.05	P	P	0.11
	207921_x_at	P	A	0.19	P	A	0.09	P	P	0.24
	207923_x_at	P	A	0.06	P	A	0.01	P	A	0.14
	207924_x_at	P	A	0.14	P	A	0.01	P	A	0.10
	209552_at	P	P	0.04	P	A	0.01	P	P	0.03
	213917_at	P	A	0.13	P	A	0.02	P	A	0.03
	214528_s_at	P	A	0.02	P	A	0.02	P	A	0.07
	221990_at	P	A	0.12	P	A	0.00	P	A	0.06
TPO	210342_s_at	P	A	0.34	P	A	0.03	P	A	0.62
TTF1	210673_x_at	P	A	0.01	P	A	0.02	P	A	0.44
	211024_s_at	P	P	0.04	P	P	0.04	P	P	0.12
CD106	203868_s_at	A	P	4.41	P	A	1.85	A	P	6.61
CD105	201808_s_at	A	A		A	A		A	A	
	201809_s_at	A	P	6.67	A	P	5.31	P	P	2.57
	228586_at	A	A		A	A		A	A	
CD90	208850_s_at	P	P	13.59	A	P	859.78	A	P	76.16
	208851_s_at	P	P	9.70	P	P	51.57	M	P	47.39
	213869_x_at	P	P	10.58	A	P	39.91	A	P	23.06
CD73	203939_at	P	P	0.83	P	P	1.27	P	P	1.50
	227486_at	P	P	1.22	P	P	1.46	P	P	1.18
	1553994_at	P	P	0.74	P	P	1.19	P	P	1.26
	1553995_a_at	P	P	0.70	P	P	1.16	P	P	1.24
KRT18	201596_x_at	P	P	0.02	P	P	0.02	P	P	0.31
Vim	201426_s_at	P	P	1.37	P	P	1.21	P	P	1.31
	1555938_x_at	P	P	0.75	P	P	1.00	P	P	0.46
E-CAD	201130_s_at	P	A	0.19	P	A	0.12	P	A	0.25
	201131_s_at	P	P	0.03	P	P	0.02	P	P	0.25

Flag score; P: present, M: marginal, A: absent.
doi:10.1371/journal.pone.0019354.t003

SAGM contains EGF, insulin, other growth factors and chemicals. These findings suggest that a particular combination of growth factors/chemicals probably changes transcriptional profiling, leading to dedifferentiation of thyrocytes.

Microarray analysis revealed that the expression of *ABCG2*, *Oct4* and *CD133* which have been used to identify stem cells in a number of tissues, were not up-regulated in the SAGM-grown cells, suggesting that the cells were a bit far from genuine pluripotent stem cells. Rather, they seem to be more committed stem/progenitor cells. In fact, mesenchymal stem cell markers *CD106*, *CD105* and *CD90* but not *CD73* were highly up-regulated. Taken together with down-regulation of *E-cadherin*, these results

suggest that the SAGM-grown cells acquired properties prior to cells committed to thyroid epithelial lineage.

GO enrichment analysis was performed and revealed differentially regulated cellular processes. Embryo implantation had the lowest p value among the up-regulated GO processes. Other up-regulated processes were endoplasmic reticulum, sterol/steroid/lipid biosynthesis/metabolic processes, cell cycle and oxidoreductase activity. These processes are generally related to protein/membrane synthesis presumably linked to cell proliferation. Regarding down-regulated GO processes, protein binding and cell adhesion processes were impacted. The down-regulation of cytoskeletal protein binding process might reflect to the loss of

Table 4. Up- or down-regulated Gene Ontology (GO) cellular processes.

(>2.0-fold)		
GO Accession	GO Term	corrected p-value
GO:0007566	embryo implantation	1.08E-05
GO:0005788 GO:0016022	endoplasmic reticulum lumen	1.33E-05
GO:0006694	steroid biosynthetic process	4.30E-04
GO:0044432	endoplasmic reticulum part	4.30E-04
GO:0005783	endoplasmic reticulum	4.30E-04
GO:0016126	sterol biosynthetic process	8.81E-04
GO:0008202	steroid metabolic process	0.004734457
GO:0008610	lipid biosynthetic process	0.008595788
GO:0016125	sterol metabolic process	0.011360187
GO:0015630	microtubule cytoskeleton	0.028312529
GO:0044444	cytoplasmic part	0.036239438
GO:0000278	mitotic cell cycle	0.039986596
GO:0016614	oxidoreductase activity, acting on CH-OH group of donors	0.053449787
GO:0016616	oxidoreductase activity, acting on the CH-OH group of donors, NAD or NADP as acceptor	0.06185003
GO:0007049	cell cycle	0.063007735
GO:0005793	ER-Golgi intermediate compartment	0.073000684
(<0.5-fold)		
GO Accession	GO Term	corrected p-value
GO:0008092	cytoskeletal protein binding	2.59E-04
GO:0007156	homophilic cell adhesion	2.59E-04
GO:0005515 GO:0045308	protein binding	0.001197793
GO:0016337	cell-cell adhesion	0.004711885

doi:10.1371/journal.pone.0019354.t004

cytokeratin-18 expression. The reduction of genes of cell adhesion process might be a consequence of the loss of epithelial property and/or polarity. It should be noted that we selected only probes scored as “present call” in all samples, which allows relatively accurate comparison of expression levels between samples. However, this means that genes with very low expression in either PT or the SAGM-grown cells were probably excluded even though their difference in expression levels was far greater.

In summary, we have developed a novel system to propagate multilineage progenitor cells from adult normal human thyroid tissues. This seems to be achieved by dedifferentiation of thyroid follicular cells without any gene delivery. Since integration of transgene(s) may cause unpredictable problem, our system has an advantage in terms of safety. The presently described culture system may be useful for regenerative medicine, but the primary importance will be as a tool to elucidate the progression of thyroid disease. Moreover, this phenomenon could be induced *in vivo* because it can be achieved without introducing foreign genes. However, as we have not confirmed full functional differentiation of the cells, further study is necessary for regenerative application.

References

- Burstein DE, Nagi C, Wang BY, Unger P (2004) Immunohistochemical detection of p53 homolog p63 in solid cell nests, papillary thyroid carcinoma, and hashimoto's thyroiditis: A stem cell hypothesis of papillary carcinoma oncogenesis. *Hum Pathol* 35: 465–473.
- Cameselle-Teijeiro J, Preto A, Soares P, Sobrinho-Simoes M (2005) A stem cell role for thyroid solid cell nests. *Hum Pathol* 36: 590–591.
- Preto A, Cameselle-Teijeiro J, Moldes-Bouloosa J, Soares P, Cameselle-Teijeiro JF, et al. (2004) Telomerase expression and proliferative activity suggest a stem cell role for thyroid solid cell nests. *Mod Pathol* 17: 819–826.
- Reis-Filho JS, Preto A, Soares P, Ricardo S, Cameselle-Teijeiro J, et al. (2003) p63 expression in solid cell nests of the thyroid: further evidence for a stem cell origin. *Mod Pathol* 16: 43–48.

Supporting Information

Figure S1 Asymmetric division of the SAGM-grown cells. A, Scheme of cell divisions. Representative data obtained by time-lapse imaging of cell cycle are shown. ACD: asymmetric cell division, SCD: symmetric cell division. 6.1% of the cells showed asymmetric division after first division. Total 198 cells were analyzed. B, Representative images after asymmetric division. (TIF)

Table S1 Time-course expression of lineage-specific markers. (PDF)

Table S2 Colony formation in SAGM after FACS. (PDF)

Author Contributions

Conceived and designed the experiments: KS NM VS YN SY. Performed the experiments: KS NM MS MM. Analyzed the data: KS NM MS MM AO AK TU HY. Contributed reagents/materials/analysis tools: KS NM VS AO AK TU HY SY. Wrote the paper: KS NM VS YN.

5. Thomas T, Nowka K, Lan L, Derwahl M (2006) Expression of endoderm stem cell markers: evidence for the presence of adult stem cells in human thyroid glands. *Thyroid* 16: 537–544.
6. Lan L, Cui D, Nowka K, Derwahl M (2007) Stem cells derived from goiters in adults form spheres in response to intense growth stimulation and require thyrotropin for differentiation into thyrocytes. *J Clin Endocrinol Metab* 92: 3681–3688.
7. Ficabracci A, Puglisi MA, Giuliani L, Mattarocci S, Gallinella-Muzi M (2008) Identification of an adult stem/progenitor cell-like population in the human thyroid. *J Endocrinol* 198: 471–487.
8. Takahashi K, Tanabe K, Ohnuki M, Narita M, Ichisaka T, et al. (2007) Induction of pluripotent stem cells from adult human fibroblasts by defined factors. *Cell* 131: 861–872.
9. Mani SA, Guo W, Liao MJ, Eaton EN, Ayyanan A, et al. (2008) The epithelial-mesenchymal transition generates cells with properties of stem cells. *Cell* 133: 704–715.
10. Santisteban M, Reiman JM, Asiedu MK, Behrens MD, Nassar A, et al. (2009) Immune-induced epithelial to mesenchymal transition in vivo generates breast cancer stem cells. *Cancer Res* 69: 2887–2895.
11. Morel AP, Lievre M, Thomas C, Hinkal G, Ansieau S, et al. (2008) Generation of breast cancer stem cells through epithelial-mesenchymal transition. *PLoS One* 3: e2888.
12. Kawabe Y, Eguchi K, Shimomura C, Mine M, Otsubo T, et al. (1989) Interleukin-1 production and action in thyroid tissue. *J Clin Endocrinol Metab* 68: 1174–1183.
13. Nakazawa Y, Saenko V, Rogounovitch T, Suzuki K, Mitsutake N, et al. (2008) Reciprocal paracrine interactions between normal human epithelial and mesenchymal cells protect cellular DNA from radiation-induced damage. *Int J Radiat Oncol Biol Phys* 71: 567–577.
14. Dimri GP, Lee X, Basile G, Acosta M, Scott G, et al. (1995) A biomarker that identifies senescent human cells in culture and in aging skin in vivo. *Proc Natl Acad Sci U S A* 92: 9363–9367.
15. Muller PY, Janovjak H, Miserez AR, Dobbie Z (2002) Processing of gene expression data generated by quantitative real-time RT-PCR. *Biotechniques* 32: 1372–1374, 1376, 1378–1379.
16. Rogakou EP, Nieves-Neira W, Boon C, Pommier Y, Bonner WM (2000) Initiation of DNA fragmentation during apoptosis induces phosphorylation of H2AX histone at serine 139. *J Biol Chem* 275: 9390–9395.
17. Schweppe RE, Klopper JP, Korch C, Pugazhenthii U, Benezra M, et al. (2008) Deoxyribonucleic acid profiling analysis of 40 human thyroid cancer cell lines reveals cross-contamination resulting in cell line redundancy and misidentification. *J Clin Endocrinol Metab* 93: 4331–4341.
18. Buley ID, Gatter KC, Heryet A, Mason DY (1987) Expression of intermediate filament proteins in normal and diseased thyroid glands. *J Clin Pathol* 40: 136–142.
19. Dockhorn-Dworniczak B, Franke WW, Schroder S, Czernobilsky B, Gould VE, et al. (1987) Patterns of expression of cytoskeletal proteins in human thyroid gland and thyroid carcinomas. *Differentiation* 35: 53–71.
20. Ramaekers F, Haag D, Jap P, Vooijs PG (1984) Immunohistochemical demonstration of keratin and vimentin in cytologic aspirates. *Acta Cytol* 28: 385–392.
21. Lehmann I, Brylla E, Sittig D, Spänel-Borowski K, Aust G (2000) Microvascular endothelial cells differ in their basal and tumour necrosis factor- α -regulated expression of adhesion molecules and cytokines. *J Vasc Res* 37: 408–416.
22. Patton WF, Yoon MU, Alexander JS, Chung-Welch N, Hechtman HB, et al. (1990) Expression of simple epithelial cytokeratins in bovine pulmonary microvascular endothelial cells. *J Cell Physiol* 143: 140–149.
23. Richter M, Tscheuschilsuren G, Eschke D, Aust G, Spänel-Borowski K, et al. (2002) Voltage-dependent potassium channels in cytokeratin-positive and cytokeratin-negative microvascular endothelial cells of the corpus luteum. *Cell Tissue Res* 310: 103–108.
24. Tscheuschilsuren G, Aust G, Nieber K, Schilling N, Spänel-Borowski K (2002) Microvascular endothelial cells differ in basal and hypoxia-regulated expression of angiogenic factors and their receptors. *Microvasc Res* 63: 243–251.
25. Matthey DL, Nixon N, Wynn-Jones C, Dawes PT (1993) Demonstration of cytokeratin in endothelial cells of the synovial microvasculature in situ and in vitro. *Br J Rheumatol* 32: 676–682.
26. Motoyama H, Ogawa S, Kubo A, Miwa S, Nakayama J, et al. (2009) In vitro reprogramming of adult hepatocytes into insulin-producing cells without viral vectors. *Biochem Biophys Res Commun* 385: 123–128.
27. Ma W, Yan RT, Li X, Wang SZ (2009) Reprogramming retinal pigment epithelium to differentiate toward retinal neurons with Sox2. *Stem Cells* 27: 1376–1387.
28. Grinnell KL, Yang B, Eckert RL, Bickenbach JR (2007) De-differentiation of mouse interfollicular keratinocytes by the embryonic transcription factor Oct-4. *J Invest Dermatol* 127: 372–380.
29. Wiese C, Rolletschek A, Kania G, Navarrete-Santos A, Anisimov SV, et al. (2006) Signals from embryonic fibroblasts induce adult intestinal epithelial cells to form nestin-positive cells with proliferation and multilineage differentiation capacity in vitro. *Stem Cells* 24: 2085–2097.
30. Ichida JK, Blanchard J, Lam K, Son EY, Chung JE, et al. (2009) A small-molecule inhibitor of *tgf-Beta* signaling replaces *sox2* in reprogramming by inducing *nanog*. *Cell Stem Cell* 5: 491–503.
31. Lyssiotis CA, Foreman RK, Staerk J, Garcia M, Mathur D, et al. (2009) Reprogramming of murine fibroblasts to induced pluripotent stem cells with chemical complementation of *Klf4*. *Proc Natl Acad Sci U S A* 106: 8912–8917.

Assessing recovery of renal function after tenofovir disoproxil fumarate discontinuation

Munehiro Yoshino · Hiroki Yagura · Hiroyuki Kushida · Hitoshi Yonemoto · Hiroki Bando · Yoshihiko Ogawa · Keishiro Yajima · Daisuke Kasai · Tomohiro Taniguchi · Dai Watanabe · Yasuharu Nishida · Takeshi Kuwahara · Tomoko Uehira · Takuma Shirasaka

Received: 3 June 2011 / Accepted: 13 September 2011

© Japanese Society of Chemotherapy and The Japanese Association for Infectious Diseases 2011

Abstract Impaired renal function caused by tenofovir disoproxil fumarate (TDF) is considered reversible by discontinuing TDF administration, but there are occasional cases of incomplete recovery. We investigated the recovery of renal function after the discontinuation of TDF. Subjects comprised patients who had been started on TDF but in whom it was later discontinued because of impaired renal function. We investigated renal function until 96 weeks after the discontinuation of TDF, and the duration of TDF administration, up to May 2010. TDF was discontinued because of impaired renal function in 21 of 766 patients (2.7%). Following discontinuation, a significant recovery was seen in eGFR ($p = 0.003$). The median duration of administration was 28 days (6–941 days) in 9 patients whose eGFR recovered to pre-administration levels, 405 days (250–1,379) in 7 patients in whom mild recovery was seen, and 1,110 days (421–1,470) in 5 patients in whom eGFR was much lower than at the time of discontinuation. A significant correlation was seen between the eGFR recovery rate and the duration of TDF administration. TDF administration was discontinued because of renal

impairment in 2.7% of patients. The duration of TDF administration was short in patients whose renal function recovered to pre-administration levels, but patients in whom sufficient recovery was not seen after discontinuation had received TDF over long periods and included many whose renal function gradually declined, even after discontinuation. Recovery of renal function after discontinuation of TDF is likely affected by the duration of TDF administration.

Keywords HIV · Antiretroviral therapy · Tenofovir · Renal function · Nephrotoxicity · Reversibility

Introduction

Tenofovir disoproxil fumarate (TDF) is recommended in the major guidelines as the first-choice nucleoside reverse transcriptase inhibitor (NRTI) that can be administered once daily [1]. However, mild and sometimes severe renal impairment have been reported in patients taking TDF [2, 3], and clear standards for discontinuation have not been defined. Renal impairment caused by TDF is thought to be reversible after the discontinuation of TDF, but cases in which renal function does not recover even after discontinuation are occasionally reported. In this study, we retrospectively investigated the recovery of renal function in patients following the discontinuation of TDF.

Patients and methods

Subjects were Japanese outpatients in the Osaka National Hospital Department of Infectious Disease who began antiretroviral therapy (ART), including TDF, by May 2010

M. Yoshino (✉) · H. Yagura · H. Kushida
Department of Pharmacy, National Hospital Organization Osaka
National Hospital, 2-1-14 Hoenzaka, Chuo-ku,
Osaka 540-0006, Japan
e-mail: yoshino@onh.go.jp

H. Yonemoto · H. Bando · Y. Ogawa · K. Yajima ·
D. Kasai · T. Taniguchi · D. Watanabe · Y. Nishida ·
T. Uehira · T. Shirasaka
AIDS Medical Center, National Hospital Organization Osaka
National Hospital, Osaka, Japan

T. Kuwahara
Department of Pharmacy, National Hospital Organization
Minami Kyoto National Hospital, Kyoto, Japan

and in whom TDF was discontinued because of renal impairment. The changes in estimated glomerular filtration rate (eGFR)¹ up to 96 weeks after discontinuation of TDF were evaluated using the Wilcoxon signed-rank test. In addition, patients discontinuing TDF administration were divided into three groups based on the eGFR recovery rate until 96 weeks after the discontinuation of TDF: (1) patients whose eGFR recovered to 100% pre-administration levels (recovery group), (2) patients whose eGFR recovered to $\geq 20\%$ of the level at the start of administration (mild recovery group), and (3) patients in whom no recovery from the level at discontinuation or exacerbation was seen (exacerbation group). The eGFR recovery rate and duration of TDF administration were investigated in these groups, and the correlation between eGFR recovery rate and duration of TDF administration was evaluated using Spearman's rank correlation test.

Results

ART including TDF was started in 766 patients; TDF caused renal impairment and was discontinued in 21 of these patients (2.7%). TDF was discontinued in all these patients because serum creatinine (sCr) had risen to abnormal levels with the administration of TDF.

The characteristics of the patients are shown in Table 1. The median age of patients in whom TDF was discontinued was 45 years (range 25–61), and included 20 men and 1 woman. TDF was the first treatment in 15 patients and the continuing treatment in 6. AIDS had developed in 13 patients. The eGFR (median) at the start of TDF administration was 74.7 mL/min/1.73 m² (range 48.1–289.3), the duration of TDF administration (median) was 57 weeks (range 1–210), and the observation period (median) after TDF discontinuation was 131 weeks (range 20–284).

Changes in eGFR for the 21 patients in whom TDF was discontinued are shown in Fig. 1. A decrease was seen from 74.7 mL/min/1.73 m² (interquartile range 65.8–83.9) to 48.3 mL/min/1.73 m² (interquartile range 45.3–54.3). After the discontinuation of TDF, eGFR recovered rapidly for 12 weeks, after which significant recovery was seen until 96 weeks. At 96 weeks after TDF administration, eGFR was 65.9 mL/min/1.73 m² (interquartile range 50.1–82.8) (vs. time of discontinuation, $p = 0.0003$). The most improved eGFR up to 96 weeks after discontinuation was 67.2 mL/min/1.73 m² (interquartile range 59.6–85.3) (vs. time of discontinuation, $p < 0.0001$).

The eGFR recovery rate until 96 weeks after the discontinuation of TDF and the duration of TDF administration are shown in Table 2. Nine patients (42.9%; recovery group) showed eGFR recovery after the discontinuation of TDF to the level seen pre-administration. Seven patients (33.3%; mild recovery group) showed eGFR recovery after discontinuation, but not to the level seen at the start of administration. Five patients (23.8%; exacerbation group) showed worsening of the eGFR after discontinuation. Changes in eGFR after discontinuation are shown in Fig. 2. The duration of TDF administration was 28 days (range 6–941 days) in the recovery group, 405 days (range 250–1,379) in the mild recovery group, and 1,110 days (range 421–1,470) in the exacerbation group. Recovery of eGFR was quicker with a shorter duration of TDF administration. Spearman's rank correlation test for eGFR recovery rate and duration of TDF administration showed a significant negative correlation ($r = -0.73$, $p = 0.0002$).

Discussion

Based on its effective anti-HIV activity and the simplicity of being taken once a day, TDF is recommended as the first-choice NRTI in major guidelines and is widely used. However, renal impairment as an adverse reaction has been reported. The renal impairment caused by TDF is thought to be an impairment in renal tubular function, but the detailed mechanism remains unknown. Tenofovir, the active component of TDF, is almost entirely eliminated unchanged in the urine, but a portion is taken up by tubular cells from the blood mainly via organic anion transporters 1 and 3 (OAT1 and OAT3), and eliminated in urine via multidrug resistant protein 4 (MRP4), a carrier protein [4]. It has been suggested that tenofovir contributes to mitochondrial toxicity in tubular cells in this transport process and leads to impairment of renal function [5, 6].

In observational studies in other countries investigating renal impairment caused by TDF, Nelson et al. reported elevated sCr of grade 1 or higher in 2.2% of patients [7], and Madeddu et al. [8] reported elevated sCr of grades 2–4 in 2.5% of patients. The incidence of renal impairment in these studies was similar to that in the Japanese patients in the present study.

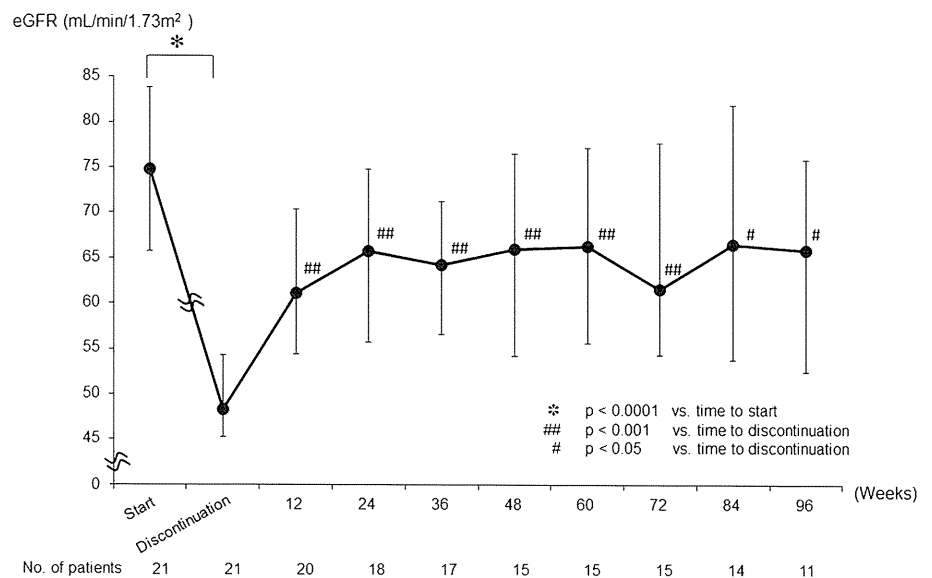
In the investigation at our hospital, there was a significant decrease in eGFR from the level at the start of administration in the 21 patients in whom TDF was discontinued compared with all patients (median: all patients 120.0 mL/min/1.73 m² vs. discontinuation patients 74.7 mL/min/1.73 m²; $p < 0.0001$). When administering TDF to patients with decreased renal function, it is advisable to select a drug after adequately evaluating renal function using eGFR or other parameters. In addition, when other causes of renal

¹ GFR calculation for Japanese (2008 Japanese Society of Nephrology calculation): $eGFR \text{ (mL/min/1.73 m}^2\text{)} = 194 \times Cr^{-1.094} \times \text{age}^{-0.287}$ (for women, $\times 0.739$).

Table 1 Characteristics of patients

Variable	No. of patients (%)	
	All patients (n = 766)	TDF discontinuation patients (n = 21)
Sex		
Male	745 (97.3)	20 (95.2)
Female	21 (2.7)	1 (4.8)
Subjects		
Naïve patients	529 (69.1)	15 (71.4)
Experienced patients	237 (30.9)	6 (28.6)
Development of AIDS	167 (21.8)	13 (61.9)
Third drug		
EFV	268 (35.0)	4 (19.0)
ATV/r	240 (31.3)	7 (33.3)
LPV/r	136 (17.8)	7 (33.3)
Others	403 (52.6)	3 (14.3)
Variable	Median (range)	
	All patients (n = 766)	TDF discontinuation patients (n = 21)
Age (years)	37 (18–73)	45 (25–61)
HIV RNA (copies/mL)	55,000 (<40–31,700,000)	95,000 (<40–3,500,000)
CD4 cell count (cells/mm ³)	205 (0–1,700)	110 (6–647)
eGFR (mL/min/1.73 m ²)	120.0 (37.4–326.7)	74.7 (48.1–289.3)
TDF duration (weeks)	107 (1–393)	57 (1–210)
Observation period after TDF discontinuation (weeks)	–	131 (20–284)

Fig. 1 Changes in eGFR (median ± interquartile range) in TDF discontinuation patients. The trend in eGFR (median ± interquartile range) after the discontinuation of TDF in 21 patients is shown



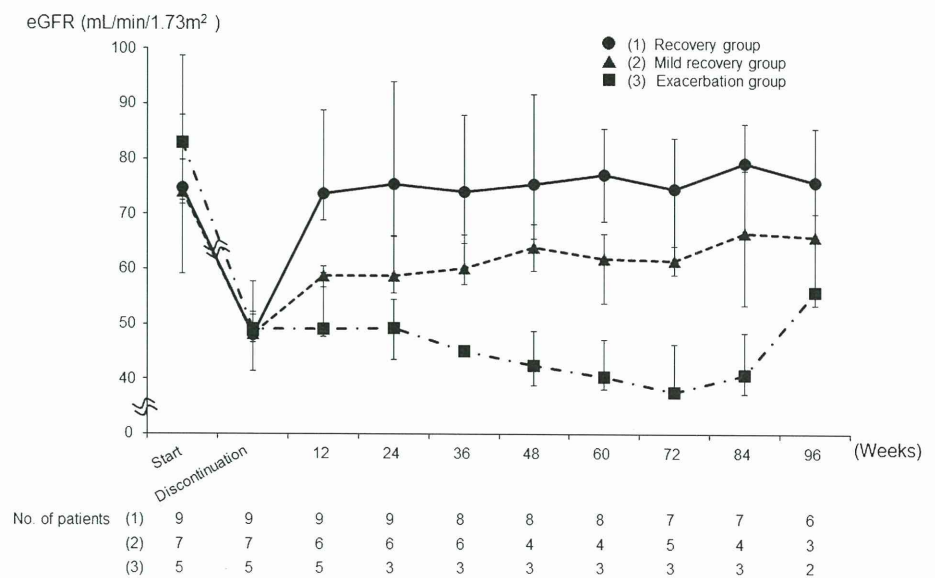
impairment were investigated in the 21 patients in whom TDF was discontinued, 13 (61.9%) had developed AIDS and received nephrotoxic drugs for treating opportunistic infections, 8 (38.1%) smoked, 5 (23.8%) had dyslipidemia, 2 (9.5%) had hypertension, and 2 (9.5%) had diabetes. Among these 21 patients, AIDS was particularly common, and it presented with *Pneumocystis jirovecii* pneumonia

(n = 8), cytomegalovirus infection (n = 3), oropharyngeal candidiasis (n = 2), progressive multifocal leukoencephalopathy (n = 2), mycobacterium tuberculosis infection (n = 1), cryptococcal infection (n = 1), and *Mycobacterium avium* complex infection (n = 1). Furthermore, the most commonly used treatment drug for these opportunistic infections was trimethoprim-sulfamethoxazole (n = 7),

Table 2 eGFR recovery rate and duration of TDF administration in TDF discontinuation patients

	No. of patients (%)	Median (interquartile range)	
		eGFR at TDF discontinuation (mL/min/1.73 m ²)	Duration of TDF administration (days)
(1) Recovery group			
Patients with 100% recovery of eGFR after TDF discontinuation	9 (42.9%)	48.1 (46.6–57.7)	28 (6–941)
(2) Mild recovery group			
Patients with mild recovery of eGFR after TDF discontinuation	7 (33.3%)	48.2 (41.4–51.7)	405 (250–1,379)
(3) Exacerbation group			
Patients with exacerbation of eGFR after TDF discontinuation	5 (23.8%)	49.2 (48.3–52.3)	1,110 (421–1,470)

Fig. 2 Changes in eGFR (median ± interquartile range) in each eGFR recovery rate group of TDF discontinuation patients. TDF discontinuation patients were divided into a recovery group (9 patients), mild recovery group (7 patients), and exacerbation group (5 patients), and the changes in eGFR (median ± interquartile range) after discontinuation are shown for each group



followed by ganciclovir and fluconazole (*n* = 4 each), rifabutin, pentamidine, sulfamethoxazole, and azithromycin (*n* = 2 each), and isoniazid, ethambutol, amikacin, and clarithromycin (*n* = 1 each). Most patients received combination therapy with 2–4 of these drugs. In AIDS patients, there is a possibility of decreased renal function both from AIDS itself and from drugs used to treat opportunistic infections; thus, sufficient caution is needed in these patients.

The renal impairment caused by TDF is thought to be reversible with the discontinuation of TDF [9–12], but in investigations using eGFR, there are patients in whom a full recovery is not seen following the discontinuation of TDF [13, 14]. In the present results, eGFR recovered rapidly for 12 weeks after discontinuation, and significant recovery was seen until 96 weeks. However, examining individual cases revealed that some patients exhibited only a mild recovery of eGFR after the discontinuation of TDF, or even exacerbated decreases in eGFR from the level at the time of discontinuation. Recovery of eGFR to the level at the start

of TDF was seen in 42.9% of patients, similar to the 42% reported by Wever et al. [14]. The fact that patients are occasionally seen in whom renal function does not recover even after discontinuation suggests the possibility that impairment of renal function may be irreversible after the discontinuation of TDF, depending on the patient.

To investigate the possible factors related to this irreversible impairment of renal function, we classified the trends in eGFR following TDF discontinuation into a recovery group, a mild recovery group, and an exacerbation group, and investigated the effect of duration of TDF administration. The recovery of eGFR was quicker with shorter durations of TDF administration. Full recovery was not seen in patients who received TDF over a long period and in whom renal function declined gradually. In 5 of 9 patients in the recovery group, renal function declined rapidly within 1 month of the start of TDF administration, and in each of these 5 cases, eGFR recovered quickly after discontinuation to the level at the start of administration.

In the mild recovery and exacerbation groups, however, none of the patients showed a rapid decline in renal function within 1 month. The decline was gradual over a long period in nearly all of these patients, and insufficient recovery or an exacerbation in eGFR was seen after discontinuation. Therefore, in patients who receive TDF over a long period, a state of gradual decline in renal function continues with accumulating damage to renal tubules from TDF, which is a likely factor in the irreversibility of damage to renal function after the discontinuation of TDF. The analysis performed in this study was done with a limited number of patients, so the factors related to irreversible damage to renal function after discontinuation of TDF could not be fully clarified. However, a correlation was confirmed between the duration of TDF administration and the eGFR recovery rate.

In recent years, Japanese and other Asians, who have a small build, have been reported to be susceptible to renal impairment caused by TDF [15, 16]. We investigated whether the recovery of renal function after the discontinuation of TDF varied depending on the eGFR equation used. No differences were observed between the eGFR equation for Japanese individuals (2008 Japanese Society of Nephrology calculation) and the eGFR equation that used a Cockcroft–Gault (CG) equation that considered the effects of body weight, and a similar trend was seen in the eGFR recovery rate after the discontinuation of TDF. On the other hand, body weight data could not be obtained at all measurement points during follow-up in the present study, and an analysis of eGFR using the CG equation and an investigation of the effects of body weight therefore could not be sufficiently conducted. In the future, it may be necessary to investigate relationships to body weight and body surface area, as well as the effects of TDF blood concentrations, in Japanese patients, who have a small build, and AIDS patients, who have a tendency to lose weight.

Our findings suggest that when discontinuation criteria for TDF are established based on sCr or eGFR, renal function may not recover following the discontinuation of TDF, particularly among patients who have received long-term administration of TDF and exhibit a gradual decline in renal function. Urinary β_2 -microglobulin and tubular reabsorption of phosphate have been reported to be useful markers for detecting renal tubular dysfunction caused by TDF at an earlier stage [13]. Because long-term administration of TDF is expected to continue in the future, it is important to investigate the use of markers that enable earlier and more sensitive detection of renal impairment caused by TDF to complement the assessment of renal function using eGFR.

With advances in treatment, HIV infection has gone from being a fatal condition to being a chronic disease that can be

managed medically. At the same time, the various side effects that accompany long-term medication are becoming clear, and measures to improve the long-term prognosis of HIV-infected patients will be an issue in the coming years. In the guidelines of the United States Department of Health and Human Services, revised January 10, 2011, the first recommendation as an NRTI is TDF/emtricitabine (FTC) alone [1]. Thus, the number of patients who continue ART including long-term TDF administration is predicted to increase, and management of renal function will be important. It is reported that approximately 30% of patients with HIV infection have pre-existing renal abnormalities, and factors in renal disease are reported to be adverse effects from anti-HIV drugs or agents to treat opportunistic infection and complications such as HIV-associated nephritis, diabetes mellitus, and hypertension [17, 18]. Given the possibility that the duration of TDF administration affects recovery from renal impairment caused by TDF, it is important when using TDF to consider the increased risk factors for concomitant diseases such as diabetes and hypertension with aging of the patient, in addition to avoiding renal impairment from drugs, such as concurrent medications. Moreover, when renal function declines gradually in patients who receive long-term administration of TDF, sufficient care must be exercised in the management of renal function and in attempts to improve the long-term outcome.

References

1. The Department of Health and Human Services. Guidelines for the use of antiretroviral agents in HIV-1-infected adults and adolescents. 2011. <http://www.aidsinfo.nih.gov/> (revised on January 10).
2. Izzedine H, Isnard-Bagnis C, Hulot JS, Vittecoq D, Cheng A, Jais CK, et al. Renal safety of tenofovir in HIV treatment-experienced patients. *AIDS*. 2004;18:1074–6.
3. Zimmermann AE, Pizzoferrato T, Bedford J, Morris A, Hoffman R, Braden G. Tenofovir-associated acute and chronic kidney disease: a case of multiple drug interactions. *Clin Infect Dis*. 2006;42:283–90.
4. Ray AS, Cihlar T, Robinson KL, Tong L, Vela JE, Fuller MD, et al. Mechanism of active renal tubular efflux of tenofovir. *Antimicrob Agents Chemother*. 2006;50:3297–304.
5. Kohler JJ, Hosseini SH, Hoying-Brandt A, Green E, Johnson DM, Russ R, et al. Tenofovir renal toxicity targets mitochondria of renal proximal tubules. *Lab Invest*. 2009;89:513–9.
6. Lebrecht D, Venhoff AC, Kirschner J, Wiech T, Venhoff N, Walker UA. Mitochondrial tubulopathy in tenofovir disoproxil fumarate-treated rats. *J AIDS*. 2009;51:258–63.
7. Nelson MR, Katlama C, Montaner JS, Cooper DA, Gazzard B, Clotet B, et al. The safety of tenofovir disoproxil fumarate for the treatment of HIV infection in adults: the first 4 years. *AIDS*. 2007;21:1273–81.
8. Madeddu G, Bonfanti P, De Socio GV, Carradori S, Grosso C, Marconi P, et al. CISA Group. Tenofovir renal safety in

- HIV-infected patients: results from the SCOLTA Project. *Biomed Pharmacother.* 2008;62:6–11.
9. Verhelst D, Monge M, Meynard JL, Fouqueray B, Mougnot B, Girard PM, et al. Fanconi syndrome and renal failure induced by tenofovir: a first case report. *Am J Kidney Dis.* 2002;40:1331–3.
 10. James CW, Steinhaus MC, Szabo S, Dressier RM. Tenofovir-related nephrotoxicity: case report and review of the literature. *Pharmacotherapy.* 2004;24:415–8.
 11. Malik A, Abraham P, Malik N. Acute renal failure and Fanconi syndrome in an AIDS patient on tenofovir treatment—case report and review of literature. *J Infect.* 2005;51:E61–5.
 12. Kapitsinou PP, Ansari N. Acute renal failure in an AIDS patient on tenofovir: a case report. *J Med Case Rep.* 2008;2:94.
 13. Kinai E, Hanabusa H. Progressive renal tubular dysfunction associated with long-term use of tenofovir DF. *AIDS Res Hum Retrovir.* 2009;25:387–94.
 14. Wever K, van Agtmael MA, Carr A. Incomplete reversibility of tenofovir-related renal toxicity in HIV-infected men. *J AIDS.* 2010;55:78–81.
 15. Chaisiri K, Bowonwatanuwong C, Kasettrat N, Kiertiburanakul S. Incidence and risk factors for tenofovir-associated renal function decline among Thai HIV-infected patients with low-body weight. *Curr HIV Res.* 2010;8:504–9.
 16. Nishijima T, Komatsu H, Gatanaga H, Aoki T, Watanabe K, Kinai E, et al. Impact of small body weight on tenofovir-associated renal dysfunction in HIV-infected patients: a retrospective cohort study of Japanese patients. *PLoS One.* 2011;6:e22661.
 17. Gupta SK, Eustace JA, Winston JA, Boydston II, Ahuja TS, Rodriguez RA, et al. Guidelines for the management of chronic kidney disease in HIV-infected patients: recommendations of the HIV Medicine Association of the Infectious Diseases Society of America. *Clin Infect Dis.* 2005;40:1559–85.
 18. Wyatt CM, Arons RR, Klotman PE, Klotman ME. Acute renal failure in hospitalized patients with HIV: risk factors and impact on in-hospital mortality. *AIDS.* 2006;20:561–5.

Outbreak of Infections by Hepatitis B Virus Genotype A and Transmission of Genetic Drug Resistance in Patients Coinfected with HIV-1 in Japan[∇]

Seiichiro Fujisaki,¹ Yoshiyuki Yokomaku,¹ Teiichiro Shiino,² Tomohiko Koibuchi,³ Junko Hattori,¹ Shiro Ibe,¹ Yasumasa Iwatani,^{1,4} Aikichi Iwamoto,³ Takuma Shirasaka,⁵ Motohiro Hamaguchi,⁶ and Wataru Sugiura^{1,4*}

Department of Infectious Diseases and Immunology, Clinical Research Center, National Hospital Organization, Nagoya Medical Center, Nagoya, Japan¹; Infectious Disease Surveillance Center, National Institute of Infectious Diseases, Tokyo, Japan²; Institute of Medical Science, The University of Tokyo, Tokyo, Japan³; Department of AIDS Research, Nagoya University Graduate School of Medicine, Nagoya, Japan⁴; AIDS Medical Center, National Hospital Organization, Osaka National Hospital, Osaka, Japan⁵; and Aichi Blood Center, Japanese Red Cross Society, Nagoya, Japan⁶

Received 24 October 2010/Returned for modification 2 December 2010/Accepted 8 January 2011

The major routes of hepatitis B virus (HBV) infection in Japan has been mother-to-child transmission (MTCT) and blood transfusion. However, HBV cases transmitted through sexual contact are increasing, especially among HIV-1-seropositive patients. To understand the molecular epidemiology of HBV in HBV/HIV-1 coinfection, we analyzed HBV genotypes and HIV-1 subtypes in HBV/HIV-1-coinfected patients at Nagoya Medical Center from 2003 to 2007. Among 394 HIV-1-infected Japanese men having sex with men (MSM) who were newly diagnosed during the study period, 31 (7.9%) tested positive for the hepatitis B virus surface antigen. HBV sequence analyses were successful in 26 cases, with 21 (80.7%) and 5 (19.3%) cases determined as genotypes A and C, respectively. Our finding that HBV genotype A was dominant in HIV-1-seropositive patients alerts clinicians to an alternative outbreak of HBV genotype A in the HIV-1-infected MSM population and a shift in HBV genotype from C to A in Japan. The narrow genetic diversity in genotype A cases suggests that genotype A has been recently introduced into the MSM population and that sexual contacts among MSM were more active than speculated from HIV-1 tree analyses. In addition, we found a lamivudine resistance mutation in one naïve case, suggesting a risk of drug-resistant HBV transmission. As genotype A infection has a higher risk than infection with other genotypes for individuals to become HBV carriers, prevention programs are urgently needed for the target population.

The number of hepatitis B virus (HBV)-infected persons in Japan is estimated to be 1 million, or 0.8% of the total population (31). HBV is classified into eight genotypes, A to H, by their differences in genome sequences (11, 12, 22). Circulating genotypes in Japan differ according to geographical region, with the prevalent genotypes in 2001 being C (84.7%) and B (12.2%), while A (1.7%) and D (0.4%) were less frequent (17). HBV infection in Japan has been transmitted mainly by two routes, mother-to-child transmission (MTCT) and blood transfusion, which have been targeted by prevention programs still being operated today (13, 15–17, 25).

Regarding MTCT, all pregnant women are screened for HBV antigen and antibody. Mothers who are HBV infected are prohibited from breast-feeding, and their newborns are vaccinated against HBV. Regarding infection by blood transfusion, all donated blood is tested by anti-hepatitis B surface antibody (HBsAb) testing and PCR to exclude HBV-contaminated blood from the supply. These prevention programs have

been successful, and the risks of HBV infection by these two routes have been reduced dramatically.

However, HBV infection by sexual contact has recently become a prevailing alternative transmission route of HBV in Japan (30, 36). In particular, coinfection with HBV and human immunodeficiency virus type 1 (HIV-1), the causative agent of AIDS, has been increasing among men who have sex with men (MSM), and the incidence of HBV infection associated with HIV-1-seropositive cases appeared to be 8.8%, which is higher than that in the general population (5). Thus, the epidemiology of HBV infection in Japan is quickly shifting. Here we report the most recent molecular epidemiologic status of HBV/HIV-1 coinfection.

MATERIALS AND METHODS

Sample. HIV/AIDS patients newly diagnosed at Nagoya Medical Center from 2003 to 2007 were tested for hepatitis B surface antigen (HBsAg), and HBsAg-positive patients were enrolled in the study. Clinical data (age, gender, suspected route of HIV-1 infection, aspartate aminotransferase [AST] and alanine aminotransferase [ALT] plasma levels, CD4-positive T cell count, and HIV viral load) were obtained from medical records. Plasma HBV viral load was measured with COBAS TaqMan (Roche Diagnostics, Basel, Switzerland), and plasma HBe IgM titer was measured with Lumipulse (Fujirebio, Tokyo, Japan). The time of HBV infection was estimated by patient interview and HBe IgM titer results. This study was conducted according to the principles expressed in the Declaration of Helsinki. The study was approved by the Institutional Review Boards of the National Institute of Infectious Diseases and Nagoya Medical Center. All pa-

* Corresponding author. Mailing address: Department of Infection and Immunology, Clinical Research Center, Nagoya Medical Center, 4-1-1 Sannomaru, Nakaku, Nagoya 4600001, Japan. Phone: 81-52-951-1111. Fax: 81-52-963-3970. E-mail: wsugiura@nnh.hosp.go.jp.

[∇] Published ahead of print on 19 January 2011.

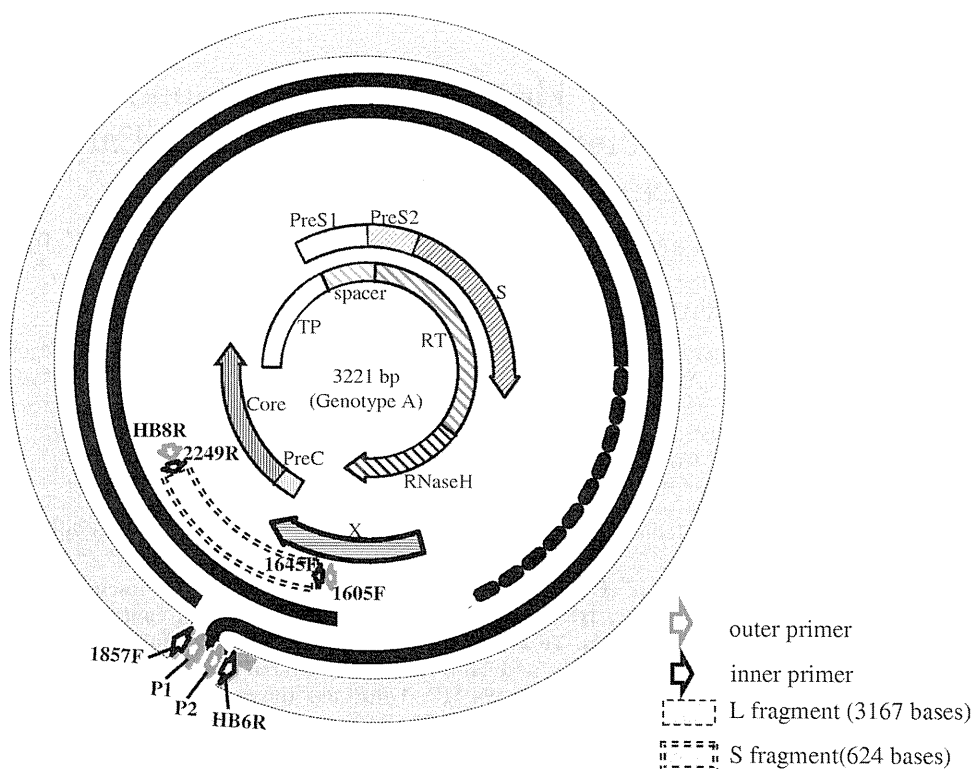


FIG. 1. Genetic regions of HBV and HIV-1 used for phylogenetic tree analyses. The whole HBV genome was amplified in two fragments, L and S, and assembled. L and S fragments are indicated by single and double dashed lines, respectively.

tients provided written informed consent for collection of samples and subsequent analysis.

Amplification of HBV and HIV DNA fragments and determination of DNA sequences. HBV nucleic acid was extracted from plasma using a MagNA Pure Compact Nucleic Acid Isolation Kit I (Roche Diagnostics). As shown in Fig. 1, the full-length HBV genome was amplified in two fragments, L (3,167 bases) and S (624 bases). The primers used for amplifying HBV DNA were both newly designed and have been published previously (27). Details of these primers are summarized in Table 1. The DNA polymerases used for the first and nested

PCRs were LA *Taq* (Takara, Shiga, Japan) and Prime Star HS (Takara) polymerase, respectively. The HBV genotypes were also determined using a commercial kit (Institute of Immunology, Tokyo, Japan) based on enzyme immunoassay to confirm that the results did not differ from those based on phylogenetic tree analysis.

The HIV-1 *gag p17* (396 bp [bp 790 to 1185]), *pol* (1,117 bp [bp 2253 to 3369]), and *env C2V3* (222 bp [bp 6996 to 7217]) regions were amplified from extracted plasma HIV-1 RNA by reverse transcription-PCR (RT-PCR) using the SuperScript one-step RT-PCR system for long templates (Invitrogen, Carlsbad, CA)

TABLE 1. Primers for amplifying the HBV and HIV-1 genomes

Name	Direction ^a	Sequence (5' → 3')	Region
P1	F	TTTTCACCTCTGCCTAATCA	First PCR, HBV L fragment
P2	R	AAAAAGTTGCATGGTGCTGG	First PCR, HBV L fragment
1605F	F	CGCATGGAGACCACCGTGAA	First PCR, HBV S fragment
HB8R	R	ATAGGGGCATTTGGTGGTCT	First PCR, HBV S fragment
1857F	F	CTACTGTTCAAGCCTCCAAG	Nested PCR, HBV L fragment
HB6R	R	AACAGACCAATTTATGCCTA	Nested PCR, HBV L fragment
1645F	R	AGGTCTTGCATAAGAGGACT	Nested PCR, HBV S fragment
2249R	F	CCAAAAGACACCAAATAYTC	Nested PCR, HBV S fragment
172A	F	ATCTCTAGCAGTGCGCCCGAACAG	RT-PCR, HIV-1 <i>gag</i> fragment
173B	R	CTGATAATGCTGAAAACATGGGTAT	RT-PCR, HIV-1 <i>gag</i> fragment
174A	F	CTCTCGACGCAGGACTCGGCTTGCT	Nested PCR, HIV-1 <i>gag</i> fragment
175B	R	CCCATGCATTCAAAGTTCTAGGTGA	Nested PCR, HIV-1 <i>gag</i> fragment
K1	F	AAGGGCTGTTGGAAATGTGG	RT-PCR, HIV-1 <i>pol</i> fragment
U13	R	CCCCTCAGGAATCCAGGT	RT-PCR, HIV-1 <i>pol</i> fragment
K4	F	GAAAGGAAGGACACCAAATGA	nested PCR, HIV-1 <i>pol</i> fragment
U12	R	CTCATTCTTGCATATTTTCTGTT	Nested PCR, HIV-1 <i>pol</i> fragment
106A	F	CATACATTATTGTGCCCCGGCTGG	RT-PCR, HIV-1 <i>env</i> fragment
17B	R	AGAAAAATTTCCCCTCTACAATTA	RT-PCR, HIV-1 <i>env</i> fragment
14A	F	AATGTCAGCTCAGTACAAATGCACAC	Nested PCR, HIV-1 <i>env</i> fragment
10B	R	ATTTCTGGGTCCCCTCTGAGG	Nested PCR, HIV-1 <i>env</i> fragment

^a F, forward; R, reverse.

TABLE 2. HBV genotype reference sequences collected from the DNA Database of Japan (DDBJ) for tMRCA analysis

Genotype	DDBJ accession no.
A.....	FJ692588, GQ325786, GQ477503, GQ477496, GQ486599, EU414132
B.....	FJ751547, GQ924611
C.....	GQ924615, GQ486096, EU939589, GQ486684
D.....	GQ486337, FJ349228, GQ924652, EU414124, GQ922001, GQ486586
E.....	GQ486756, GQ161830, FJ349237
F.....	GQ486537, GQ486515, GQ486570
G.....	GQ486843
H.....	GQ486592, AB266536

followed by a second PCR using LA *Taq* polymerase. The primers used for HIV-1 sequencing are also summarized in Table 1. The amplicons were purified using a MultiScreen PCR filter plate (Millipore, Billerica, MA), and the sequencing reaction was performed using the BigDye Terminator v3.1 cycle sequencing kit (Applied Biosystems, Carlsbad, CA) and analyzed with the ABI PRISM 3130 (Applied Biosystems) autosequencer. Electropherograms were edited and verified by SeqScape v2.5 software (Applied Biosystems).

Phylogenetic tree analyses and genotype determination. HBV genotypes were determined by phylogenetic tree analysis with reference sequences. HBV sequences were aligned with 23 reference sequences from the National Center for Biotechnology Information (NCBI) database by using the CLUSTAL W program and analyzed by Kimura two-parameter methods. Genetic distances were calculated by the maximum composite likelihood, and phylogenetic trees were constructed by the neighbor-joining method using MEGA version 4 software. The reliabilities of branches were evaluated by bootstrap analysis with 1,000 replicates.

Phylogenetic trees of the HIV-1 *gag*, *pol*, and *env* regions were also constructed with 62 HIV-1 reference sequences obtained from the HIV-1 sequence database (Los Alamos National Laboratory).

Estimated tMRCAs. Evolutionary rates, chronological phylogenies, and other evolutionary parameters of HBV genotypes were estimated from heterochronous data for the HBV genomic sequences collected in our study, together with reference sequences from public databases (Table 2), using the Bayesian Markov chain Monte Carlo (MCMC) method. The nucleotide substitution model was evaluated by the hierarchical likelihood ratio test using PAUP v4.0 (29) with MrModeltest (14) and the general time-reversible (GTR) model with both invariant site (I) and gamma-distributed site (G) heterogeneity for four rate categories showing maximum likelihood. Bayesian MCMC analyses were performed with BEAST v1.4.8 (4) using the substitution model of GTR + I + G, three partitions into codon positions, and a relaxed molecular clock model (the uncorrelated log normal-distributed model) (3). Four different population dynamic models (exponential growth, logistic growth, constant population, and Bayesian skyline plot [BSP]) were tested in the analyses. According to BSP properties, constant-growth models were adopted for the HBV genome sequences. Each Bayesian MCMC analysis was run for 40 million states and sampled every 10,000 states. Posterior probabilities were calculated with a burn-in of 4 million states and checked for convergence using Tracer v1.4 (21). The maximum clade credibility tree for analyzing the MCMC data set was annotated by TreeAnnotator in the BEAST package. The posterior distribution of the substitution rate obtained from the heterochronous sequences was subsequently incorporated as a prior distribution for the mean evolutionary rate of the HBV genome, thereby adding a time scale to the phylogenetic histories of the given viruses and enabling estimation of the time of the most recent common ancestor (tMRCA) (19).

Determination of HBV drug resistance mutations. HBV cases resistant to nucleoside analogue reverse transcriptase inhibitors (NRTI) were determined by analyzing amino acid sequences of the RT region. The approved anti-HBV drugs in Japan are lamivudine, adefovir, and entecavir. In cases of HBV/HIV-1 coinfection, tenofovir and emtricitabine are also used. We studied whether the viruses have drug resistance mutations against these antiretroviral drugs with or without a history of antiretroviral treatments and confirmed the following resistance mutations: lamivudine/emtricitabine resistance mutations V173L, L180M, and M204I/V; adefovir resistance mutations A181V, I233V, and N236T; entecavir resistance mutations I169T, L180M, T184G, S202I, M204I/V, and M250V; and tenofovir resistance mutation A194T (1, 2, 24, 32, 34, 35). Furthermore, major drug resistance mutations in HIV-1 were defined according to the criteria

of the International AIDS Society (IAS)-USA and Stanford HIV drug resistance database (7, 23).

RESULTS

The major HBV genotype circulating among Japanese MSM is genotype A. During the study period, 394 cases were newly diagnosed as HIV/AIDS, and 31 cases were determined as HBsAg positive. Thus, the average prevalence of HBV/HIV-1 coinfection in our study population was 7.9%. Analysis of the coinfection prevalence in each year showed increases from 2.8 to 3.3% in 2003 to 2004 and from 7.4 to 13.2% in 2005 to 2007 (Fig. 2). As the suspected route of HIV-1 infections in all 31 cases was MSM, HBV appears to be quickly spreading among the MSM population. Of these HBV/HIV-1-coinfected cases, 26 isolates were successfully sequenced for both HBV and HIV-1, and their subtypes and genotypes were determined. Regarding the five cases for which the HBV genome could not be sequenced, plasma HBV DNA copies were undetectable in four cases, and low (10^{3-3} copies/ml) in one case.

The median age of the patients was 34 years (interquartile range [IQR], 29.5 to 37.0) (Table 3). The median plasma viral loads of HBV and HIV-1 were 4.4×10^8 (IQR, $4.9 \times 10^4 - 6.3 \times 10^8$) and 6.4×10^4 (IQR, $2.0 \times 10^4 - 2.0 \times 10^5$) copies/ml, respectively. Hepatitis B core antigen (HBcAg) IgM was positive in nine patients, of which two were suspected to harbor acute HBV infection according to their HBsAg positivity, AST and ALT plasma levels, and patient interviews. The other 7 HBcAg-positive patients were categorized as having acute hepatitis or exacerbated chronic hepatitis, and 17 HBcAg-negative patients were determined as being in the chronic hepatitis stage.

According to phylogenetic tree analysis, 26 cases were classified into two genotypes, either A or C. As shown in Fig. 3, 21 and 5 cases were classified as genotypes A and C, respectively. The subgenotypes of the 21 genotype A cases were all A2, the predominant subgenotype in Europe and North America, whereas the subgenotypes of the 5 genotype C cases were all C1, the most prevalent subgenotype in eastern Asia, including Japan, South Korea, and northern China. Genotype B, the

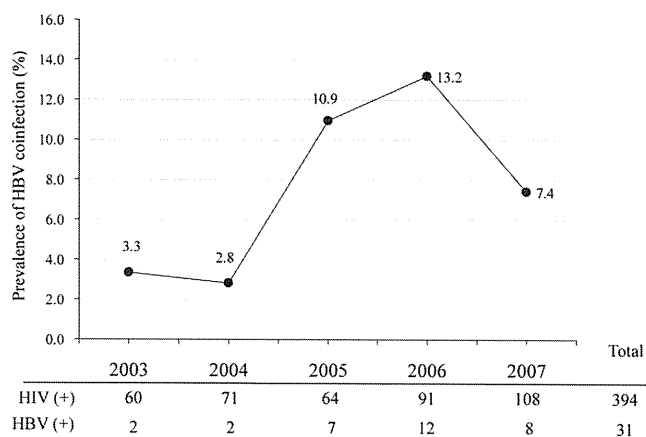


FIG. 2. Transitions in HBV infection rates in HBV/HIV-1-coinfected patients. HBV infection rates are plotted versus year, with the numbers of HIV-1-infected and HBV/HIV-1-coinfected patients shown below the x axis.

TABLE 3. Characteristics of HBV/HIV-1-coinfected patients

Characteristic	Value ^a for genotype:			P
	All (n = 26)	A (n = 21)	C (n = 5)	
Age (yr)	34 (30–37)	33 (29–37)	56 (46–57)	<0.01
Suspected route of HIV-1 infection	MSM	MSM	MSM	
AST (IU/liter)	31 (26–63)	29 (26–48)	54 (20–74)	
ALT (IU/liter)	43 (33–90)	42 (32–85)	44 (34–99)	
No. HBcAg IgM positive	9	9	0	
CD4 (/μl)	293 (91–492)	300 (94–484)	202 (9–494)	<0.01
HIV-1 viral load (copies/ml)	6.4 × 10 ⁴ (2.0 × 10 ⁴ –2.0 × 10 ⁵)	6.8 × 10 ⁴ (2.4 × 10 ⁴ –2.1 × 10 ⁵)	2.4 × 10 ⁴ (2.4 × 10 ² –9.7 × 10 ⁴)	
HBV viral load (copies/ml)	4.4 × 10 ⁸ (4.9 × 10 ⁴ –6.3 × 10 ⁸)	6.3 × 10 ⁸ (4.7 × 10 ⁴ –6.3 × 10 ⁸)	2.0 × 10 ⁸ (4.7 × 10 ⁵ –6.3 × 10 ⁸)	

^a Median values are shown. Numbers in parentheses represent interquartile ranges.

second most predominant HBV genotype in Japan, was not detected in our study. Interestingly, the genotype A and C populations showed obvious differences in genetic diversity. The 21 group A2 samples (Fig. 3) formed a cluster with little

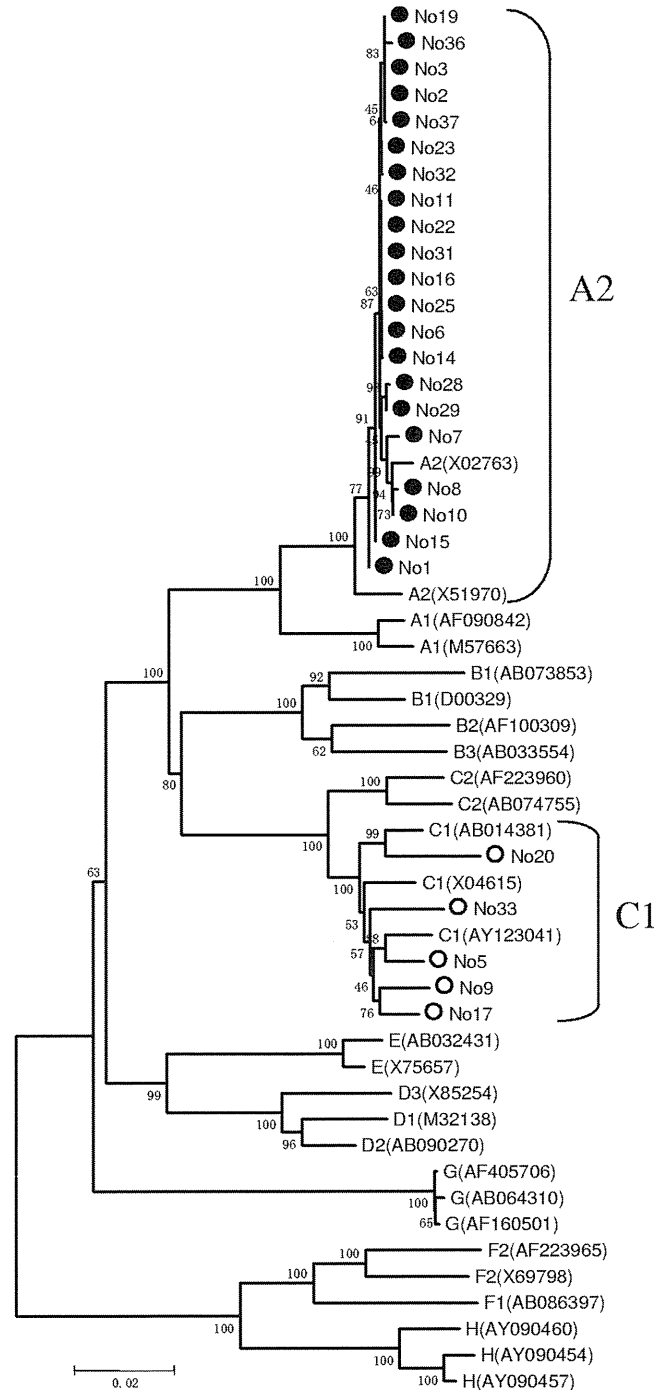


FIG. 3. Phylogenetic tree analyses of HBV isolated from HBV/HIV-1-coinfected patients. The phylogenetic tree was constructed using 26 full-length HBV genome sequences detected in HBV/HIV-1-coinfected patients in Nagoya (both solid and open circles) and 23 reference sequences from the NCBI database. Twenty-one and five cases were distributed in the clusters of genotype A (solid circles) and C (open circles), respectively.

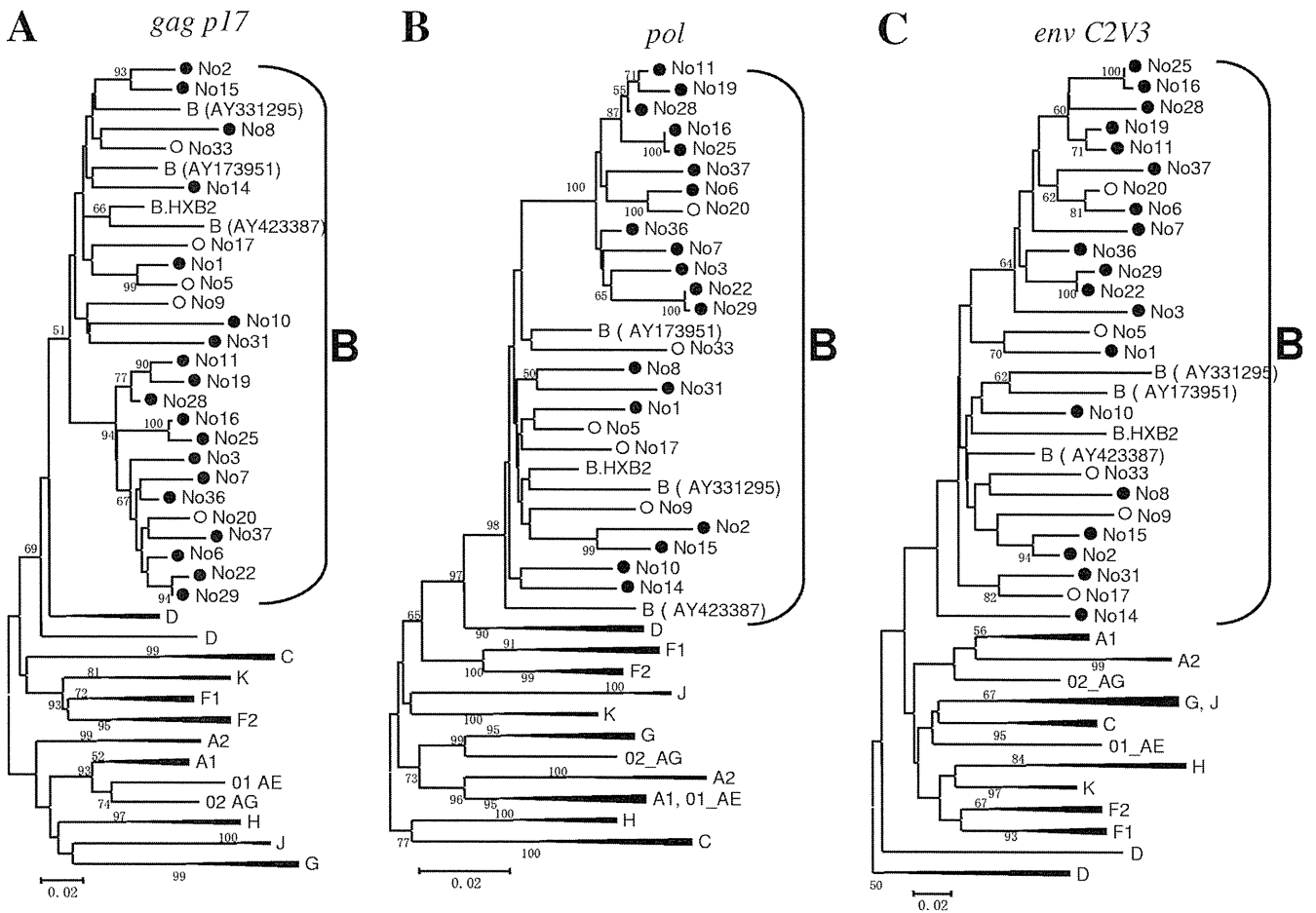


FIG. 4. Phylogenetic tree analyses of HIV-1 isolated from HBV/HIV-1-coinfecting patients. Phylogenetic trees were constructed using the 25 HIV-1 sequences obtained in this study and 62 HIV-1 reference sequences from the Los Alamos National Laboratory database. The nucleotide base sequences of *gag p17* (A), *pol* PR to RT (B), and *env C2V3* (C) gene regions were analyzed. In all analyses, all the HIV-1-positive cases detected in Nagoya (both solid and open circles) were distributed in the subtype B cluster. Cases of coinfection with genotype C HBV are shown with open circles.

or no genetic distance between each other, indicating their extremely close genetic relationships. In contrast, the five group C1 cases did not form a single cluster and had longer branches than those of group A2.

Patients with genotypes A and C also differed significantly in age (Table 3). The median age of the genotype A patients was 33 years (IQR, 29 to 37), whereas that of the genotype C patients was 56 (IQR, 46 to 57) ($P < 0.01$). Furthermore, all nine HBcAg IgM-positive cases, including five suspected cases of acute infection, were categorized in genotype A2, suggesting ongoing active transmission of the virus among the Japanese MSM population. Thus, the genotype A2 population appeared to be younger, with more acute cases, and infected with an almost genetically identical HBV strain. These two genotypes did not differ significantly in regard other clinical data, such as AST and ALT levels, CD4⁺ T cell count, and HBV and HIV-1 viral loads.

To clarify the detailed epidemiological features of HBV/HIV-1-coinfecting patients, the HIV-1 subtypes and their genetic distances were determined by phylogenetic analyses of three genome regions, *gag p17*, *pol*, and *env C2V3*. All 26 samples were determined as subtype B (Fig. 4A, B, and C), and

interestingly, branch patterns and relationships among cases were different from those for HBV. There were six paired cases, demonstrating a significantly close genetic relationship (>50% bootstrap value) in more than two regions. These paired cases were cases 1 and 5, 2 and 15, 6 and 20, 11 and 19, 16 and 25, and 22 and 29, and these connections were not evident in the HBV phylogeny, suggesting different origins of sexual partner between the two pathogens in each pair. An alternative explanation could be that little genetic variation in HBV made it difficult to clarify the genetic relationships between cases. However, there was one discordant pair (cases 1 and 5); one case had HBV genotype A, and the other case had HBV genotype C. Furthermore, the other four HBV genotype C2 cases (cases 9, 17, 20, and 33) were scattered among HIV-1 phylogenies within genotype B HIV-1-infected patients.

HBV strains detected in HIV-1-infected patients from Nagoya are the same viruses found in other parts of Japan. To clarify whether the dominance of genotype A HBV in HIV-1-infected MSM is a regional issue in the Nagoya urban area or a more nationwide epidemic, we reconstructed an HBV phylogenetic tree of 26 cases together with HBV sequences col-

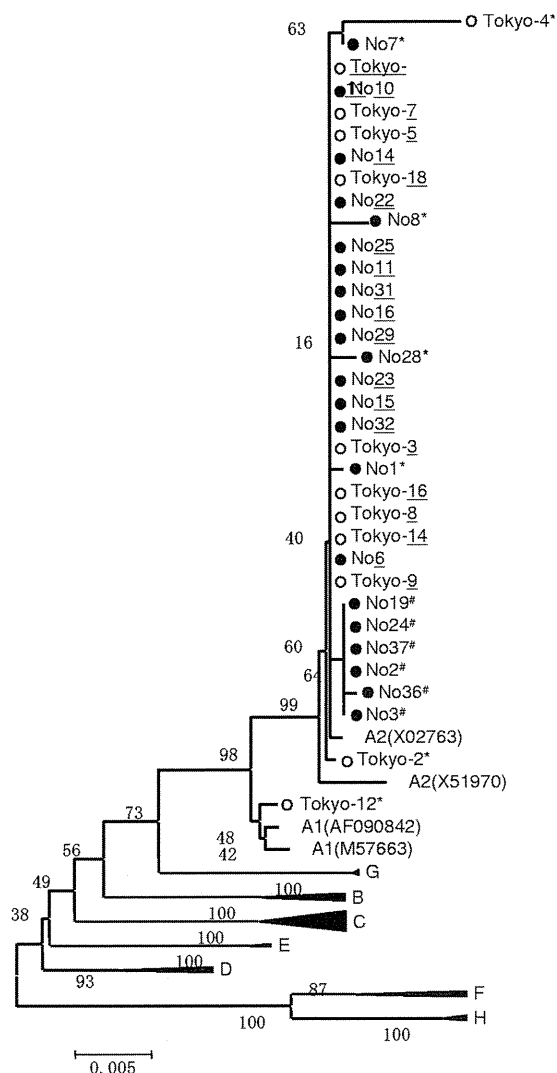


FIG. 5. Phylogenetic tree analysis of 35 HBV region S sequences, 22 from Nagoya (solid circles) and 13 from Tokyo (open circles). Three genetically different groups are indicated by asterisks, pound signs, and underlining.

lected at a different time and from a different area of Japan, i.e., 12 genotype A sequences from HBV/HIV-1-coinfected patients collected in Tokyo about 10 years before this study (8). As no full genome sequences were available for the Tokyo cases, only the S gene (681 bp [bp 155 to 835]) was analyzed. From the phylogenetic tree pattern, genotype A was classified into three groups (Fig. 5). The first is a group of 21 identical sequences (underlined in Fig. 5). As this group had the largest number of cases and included sequences from both Nagoya and Tokyo, this strain appears to be prevailing nationwide. The second group is a cluster of cases, i.e., cases 2, 3, 19, 24, 36, and 37. As all six cases were from Nagoya, this isolate still seems to be in an endemic status. The third group comprises isolates with longer branches (noted by asterisks), i.e., Tokyo-2, -4, and -12 and Nagoya-1, -7, -8, and -28. These isolates appear to be quite distinct from the others, suggesting that their origin may not be sexual contact but another route, such as MTCT or transfusions.

The prevailing HBV genotype A2 emerged more recently than most other genotypes. To estimate the emergence time of the prevailing genotype A2 strain, we estimated its mutation rate per year and tMRCA. First, the median mutation rate per year was calculated as 3.23×10^{-5} (5.62×10^{-8} to 9.01×10^{-5}), which is close to those previously reported (10, 18). Next, the median tMRCA of all A strains, A1, A2, and C were determined to be 370.8, 88.9, 184.3, and 494.9 years ago, respectively (Table 4; Fig. 6). Thus, the A2 genotype is one of the youngest HBV genotypes.

A lamivudine resistance amino acid HBV mutation detected in an antiretroviral therapy-naïve patient. We clarified not only HBV genotypes but also the incidence of transmitted drug-resistant HBV among the study patients. Analysis of the amino acid sequence of the HBV RT region showed a combined triple amino acid mutation, rtV173L + rtL180M + rtM204V, which was a mutation causing resistance against lamivudine and its 5-fluoro analogue (2',3'-dideoxy-3'-thia-5-fluorocytidine), in two patients (patients 5 and 8). However, one patient (patient 5) had been treated with stavudine-lamivudine-efavirenz at the time of sample collection, and thus only one case (case 8) was suspected to be a transmitted HBV drug-resistant case. No HIV-1 drug-resistant virus transmission was detected in the study sample.

DISCUSSION

This molecular epidemiological study of HBV infection in HIV-1-seropositive patients revealed epidemiological characteristics that were unique compared to those of the general population in Japan. All HBV/HIV-1-coinfected patients were MSM, they had a 10-fold-higher prevalence (7.9%) than that of the general population, and genotype A was the predominant HBV genotype (31). This distinct HBV epidemic in MSM was first reported in 2001 in other regions of the country (9, 36), a decade before our study. Furthermore, phylogenetic analysis of sequences from the two studies, collected in different regions and years, revealed that an identical genotype A strain prevails among the MSM population nationwide.

Considering the status of HBV epidemiology in the general population of Japan, genotypes C and B must have an equal or greater chance to disseminate among the HIV-1-seropositive

TABLE 4. Estimated times of the most recent ancestor (tMRCA) for HBV genotypes

Genotype	Mean tMRCA (yr before)		95% HPD ^a	
	Mean	Median	L	H
A	1,294.2	370.8	27.1	4,046.4
A1	306.6	88.9	12.4	976.4
A2	597.4	184.3	18.8	1,886.2
B	345.8	88.5	4.2	1,069.3
C	1,655.3	494.9	36.6	5,124.7
D	1,062.4	308.6	20.8	3,296.6
E	827.2	226.6	11.2	2,469.4
F	163.7	38.9	4.5	539.7
H	1,060.8	308.2	13.7	3,277.4
	433.8	110.1	5.6	1,303.0

^a HPD, highest posterior density.

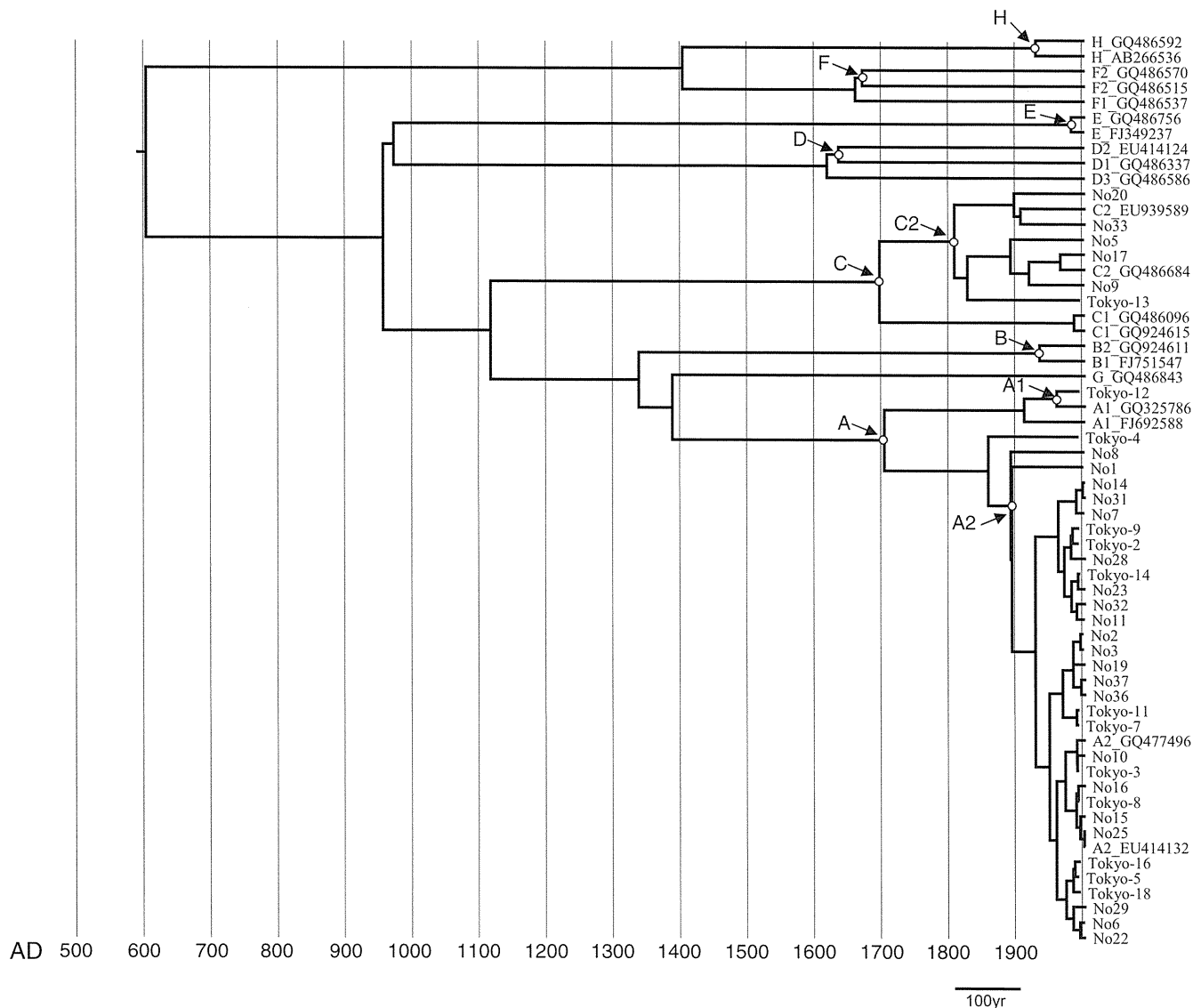


FIG. 6. Maximum clade credibility tree depicted according to median tMRCA. Nodes with open circles are evaluated points for each genotype summarized in Table 2.

MSM population. In fact, we found five genotype C patients in our study sample, and all five patients were MSM. However, because these five genotype C patients were older and their isolates had longer branches in phylogenetic analysis than the prevailing genotype A isolates, they appear to have been independently infected through either MTCT or blood transfusion events rather than sexual contact. Furthermore, as all five cases were singletons without any genetically close isolates among the samples analyzed, this genotype appeared to be less efficiently transmitted by sexual contact.

Interestingly, predominant genotype A HBV coinfection in HIV-seropositive MSM populations has also been reported in European and South American countries (20, 26, 33), suggesting that the prevailing genotype A in HIV-seropositive MSM has become a worldwide HBV epidemic. Regarding HBV genotypes in the HIV-negative population in Japan, genotype A has been increasing, but the major HBV

genotype is still C, with genotype A remaining at 3.5% nationwide and 2.1% in the Tokai area, which includes Nagoya city (9). Therefore, the prevalence of genotype A HBV in the MSM population is significantly higher than in the rest of the population.

Thus, it is interesting to discuss the virological advantages disposing this genotype A isolate to become the major player in HBV/HIV-1 coinfection among MSM. One such advantage might be the higher progression rate (16 to 23%) to chronicity of genotype A than of genotype C (28, 30), enhancing its capacity to serve as a source of new infections. As 9 of 26 genotype A-infected patients (35%) were HBcAg IgM positive and 2 had acute hepatitis, it is obvious that genotype A infections are actively ongoing among the MSM population. Though further studies are needed, considering the tMRCA of the prevailing strain A2, the younger age of patients infected with this strain than of those infected with other genotypes,

and its high prevalence among MSM, this strain may have acquired higher infectivity and efficient transmission through sexual contact.

Another issue we wanted to clarify in this study was the transmission of antiviral drug resistance. We found no antiretroviral resistance in the 26 sequenced cases. On the other hand, we detected two cases with a mutation combination of rtV173L + rtL180M + rtM204V in HBV reverse transcriptase, demonstrating resistance against lamivudine-emtricitabine. One patient was antiretroviral therapy naïve; thus, transmission of drug-resistant HBV is strongly suspected. It is peculiar that the isolate harboring the drug-resistant mutations in HBV was a singleton, considering that genetically identical isolates were prevailing, that there were very low mutation rates that suggest few chances of reverting to wild type, and that there were actively ongoing *de novo* infections. This finding might be due to resistant viruses being masked by wild-type viruses under untreated conditions, as reported in the case of HIV-1 drug resistance (6). The possibility of minority resistance populations of HBV could be verified by detection with a highly sensitive method.

In conclusion, we clarified the molecular epidemiology of HBV/HIV-1 coinfection in Japan. Our data suggest that ongoing HBV infections lie outside prevention programs targeting the MTCT and blood transfusion infection routes, and they suggest the urgent need for new prevention strategies focusing on the high-risk group of the HIV-1-seropositive MSM population.

ACKNOWLEDGMENTS

This study was supported by a Research Grant for Research on HIV/AIDS from the Ministry of Health, Labor, and Welfare of Japan (no. H19-AIDS-007, H21-AIDS-005, and H22-AIDS-004).

We thank Yasuhito Tanaka, Nagoya City University Graduate School of Medical Sciences, for helpful discussion and Claire Baldwin for help in preparing the manuscript.

REFERENCES

- Allen, M. I., et al. 1998. Identification and characterization of mutations in hepatitis B virus resistant to lamivudine. Lamivudine Clinical Investigation Group. *Hepatology* **27**:1670–1677.
- Angus, P., et al. 2003. Resistance to adefovir dipivoxil therapy associated with the selection of a novel mutation in the HBV polymerase. *Gastroenterology* **125**:292–297.
- Drummond, A. J., S. Y. Ho, M. J. Phillips, and A. Rambaut. 2006. Relaxed phylogenetics and dating with confidence. *PLoS Biol.* **4**:e88.
- Drummond, A. J., and A. Rambaut. 2007. BEAST: Bayesian evolutionary analysis by sampling trees. *BMC Evol. Biol.* **7**:214.
- Gatanaga, H., et al. 2007. Drug-resistant HIV-1 prevalence in patients newly diagnosed with HIV/AIDS in Japan. *Antiviral Res.* **75**:75–82.
- Harrigan, P. R., S. Bloor, and B. A. Larder. 1998. Relative replicative fitness of zidovudine-resistant human immunodeficiency virus type 1 isolates in vitro. *J. Virol.* **72**:3773–3778.
- Johnson, V. A., et al. 2009. Update of the drug resistance mutations in HIV-1: December 2009. *Top. HIV Med.* **17**:138–145.
- Koibuchi, T., et al. 2001. Predominance of genotype A HBV in an HBV-HIV-1 dually positive population compared with an HIV-1-negative counterpart in Japan. *J. Med. Virol.* **64**:435–440.
- Matsuura, K., et al. 2009. Distribution of hepatitis B virus genotypes among patients with chronic infection in Japan shifting toward an increase of genotype A. *J. Clin. Microbiol.* **47**:1476–1483.
- Michitaka, K., et al. 2006. Tracing the history of hepatitis B virus genotype D in western Japan. *J. Med. Virol.* **78**:44–52.
- Miyakawa, Y., and M. Mizokami. 2003. Classifying hepatitis B virus genotypes. *Intervirology* **46**:329–338.
- Norder, H., et al. 2004. Genetic diversity of hepatitis B virus strains derived worldwide: genotypes, subgenotypes, and HBsAg subtypes. *Intervirology* **47**:289–309.
- Noto, H., et al. 2003. Combined passive and active immunoprophylaxis for preventing perinatal transmission of the hepatitis B virus carrier state in Shizuoka, Japan during 1980–1994. *J. Gastroenterol. Hepatol.* **18**:943–949.
- Nylander, J. 2004. MrModeltest v2. Uppsala University, Uppsala, Sweden.
- Oda, T. 2000. Further decline of hepatitis B surface antigen (HBsAg) prevalence in Japan. *Jpn. J. Cancer Res.* **91**:361.
- Okada, K., I. Kamiyama, M. Inomata, M. Imai, and Y. Miyakawa. 1976. e antigen and anti-e in the serum of asymptomatic carrier mothers as indicators of positive and negative transmission of hepatitis B virus to their infants. *N. Engl. J. Med.* **294**:746–749.
- Orito, E., et al. 2001. Geographic distribution of hepatitis B virus (HBV) genotype in patients with chronic HBV infection in Japan. *Hepatology* **34**:590–594.
- Osiowy, C., E. Giles, Y. Tanaka, M. Mizokami, and G. Y. Minuk. 2006. Molecular evolution of hepatitis B virus over 25 years. *J. Virol.* **80**:10307–10314.
- Pybus, O. G., A. J. Drummond, T. Nakano, B. H. Robertson, and A. Rambaut. 2003. The epidemiology and iatrogenic transmission of hepatitis C virus in Egypt: a Bayesian coalescent approach. *Mol. Biol. Evol.* **20**:381–387.
- Quarleri, J., et al. 2007. Hepatitis B virus genotype distribution and its lamivudine-resistant mutants in HIV-coinfected patients with chronic and occult hepatitis B. *AIDS Res. Hum. Retroviruses* **23**:525–531.
- Rambaut, A., and A. J. Drummond. 2007. Tracer v1.4. Institute of Evolutionary Biology, University of Edinburgh, Edinburgh, Scotland. <http://tree.bio.ed.ac.uk>.
- Schaefer, S. 2007. Hepatitis B virus taxonomy and hepatitis B virus genotypes. *World J. Gastroenterol.* **13**:14–21.
- Shafer, R. 2010, posting date. Stanford drug resistance database. <http://hivdb.stanford.edu/>.
- Sheldon, J., et al. 2005. Selection of hepatitis B virus polymerase mutations in HIV-coinfected patients treated with tenofovir. *Antivir. Ther.* **10**:727–734.
- Shiraki, K. 2000. Perinatal transmission of hepatitis B virus and its prevention. *J. Gastroenterol. Hepatol.* **15**(Suppl.):E11–E15.
- Soriano, V., et al. 2010. Predictors of hepatitis B virus genotype and viraemia in HIV-infected patients with chronic hepatitis B in Europe. *J. Antimicrob. Chemother.* **65**:548–555.
- Sugauchi, F., et al. 2001. A novel variant genotype C of hepatitis B virus identified in isolates from Australian Aborigines: complete genome sequence and phylogenetic relatedness. *J. Gen. Virol.* **82**:883–892.
- Suzuki, Y., et al. 2005. Persistence of acute infection with hepatitis B virus genotype A and treatment in Japan. *J. Med. Virol.* **76**:33–39.
- Swafford, D. 2003. PAUP. Phylogenetic analysis using parsimony (and other methods), version 4. Sinauer Associates, Sunderland, MA.
- Takeda, Y., et al. 2006. Difference of HBV genotype distribution between acute hepatitis and chronic hepatitis in Japan. *Infection* **34**:201–207.
- Tanaka, J., et al. 2004. Sex- and age-specific carriers of hepatitis B and C viruses in Japan estimated by the prevalence in the 3,485,648 first-time blood donors during 1995–2000. *Intervirology* **47**:32–40.
- Tenney, D. J., et al. 2004. Clinical emergence of entecavir-resistant hepatitis B virus requires additional substitutions in virus already resistant to lamivudine. *Antimicrob. Agents Chemother.* **48**:3498–3507.
- Trimoulet, P., et al. 2007. Hepatitis B virus genotypes: a retrospective survey in southwestern France, 1999–2004. *Gastroenterol. Clin. Biol.* **31**:1088–1094.
- Westland, C. E., et al. 2003. Week 48 resistance surveillance in two phase 3 clinical studies of adefovir dipivoxil for chronic hepatitis B. *Hepatology* **38**:96–103.
- Yang, H., et al. 2002. Resistance surveillance in chronic hepatitis B patients treated with adefovir dipivoxil for up to 60 weeks. *Hepatology* **36**:464–473.
- Yotsuyanagi, H., et al. 2005. Distinct geographic distributions of hepatitis B virus genotypes in patients with acute infection in Japan. *J. Med. Virol.* **77**:39–46.

ORIGINAL ARTICLE

Pre-transplant imatinib-based therapy improves the outcome of allogeneic hematopoietic stem cell transplantation for *BCR-ABL*-positive acute lymphoblastic leukemia

S Mizuta¹, K Matsuo², F Yagasaki³, T Yujiri⁴, Y Hatta⁵, Y Kimura⁶, Y Ueda⁷, H Kanamori⁸, N Usui⁹, H Akiyama¹⁰, Y Miyazaki¹¹, S Ohtake¹², Y Atsuta¹³, H Sakamaki¹⁰, K Kawa¹⁴, Y Morishima¹⁵, K Ohnishi¹⁶, T Naoe¹⁷ and R Ohno¹⁸

¹Department of Hematology, Fujita Health University Hospital, Toyoake, Japan; ²Division of Epidemiology and Prevention, Aichi Cancer Center Research Institute, Nagoya, Japan; ³Department of Hematology, Saitama Medical University International Medical Center, Saitama, Japan; ⁴Third Department of Internal Medicine, Yamaguchi University School of Medicine, Ube, Japan; ⁵Department of Hematology, Nihon University School of Medicine, Tokyo, Japan; ⁶Division of Hematology, First Department of Internal Medicine, Tokyo Medical University, Tokyo, Japan; ⁷Department of Hematology/Oncology, Kurashiki Central Hospital, Kurashiki, Japan; ⁸Department of Hematology, Kanagawa Cancer Center, Yokohama, Japan; ⁹Department of Clinical Oncology and Hematology, Jikei University Daisan Hospital, Tokyo, Japan; ¹⁰Department of Hematology, Tokyo Metropolitan Cancer and Infectious Diseases Center, Komagome Hospital, Tokyo, Japan; ¹¹Department of Hematology, Nagasaki University School of Medicine, Nagasaki, Japan; ¹²Department of Clinical Laboratory Science, Kanazawa University Graduate School of Medical Science, Kanazawa, Japan; ¹³Department of Hematopoietic Stem Cell Transplantation Data Management/Biostatistics, Nagoya University Graduate School of Medicine, Nagoya, Japan; ¹⁴Division of Hematology and Oncology, Osaka Medical Center and Research Institute for Maternal and Child Health, Izumi, Japan; ¹⁵Department of Hematology and Cell Therapy, Aichi Cancer Center Hospital, Nagoya, Japan; ¹⁶Oncology Center, Hamamatsu University School of Medicine, Hamamatsu, Japan; ¹⁷Department of Hematology and Oncology, Nagoya University Graduate School of Medicine, Nagoya, Japan and ¹⁸President Emeritus, Aichi Cancer Center, Nagoya, Japan

A high complete remission (CR) rate has been reported in newly diagnosed Philadelphia chromosome-positive acute lymphoblastic leukemia (Ph+ALL) following imatinib-based therapy. However, the overall effect of imatinib on the outcomes of allogeneic hematopoietic stem cell transplantation (allo-HSCT) is undetermined. Between 2002 and 2005, 100 newly diagnosed adult patients with Ph+ALL were registered to a phase II study of imatinib-combined chemotherapy (Japan Adult Leukemia Study Group Ph+ALL202 study) and 97 patients achieved CR. We compared clinical outcomes of 51 patients who received allo-HSCT in their first CR (imatinib cohort) with those of 122 historical control patients in the pre-imatinib era (pre-imatinib cohort). The probability of overall survival at 3 years after allo-HSCT was 65% (95% confidence interval (CI), 49–78%) for the imatinib cohort and 44% (95% CI, 35–52%) for the pre-imatinib cohort. Multivariate analysis confirmed that this difference was statistically significant (adjusted hazard ratio, 0.44, $P=0.005$). Favorable outcomes of the imatinib cohort were also observed for disease-free survival ($P=0.007$) and relapse ($P=0.002$), but not for non-relapse mortality ($P=0.265$). Imatinib-based therapy is a potentially useful strategy for newly diagnosed patients with Ph+ALL, not only providing them more chance to receive allo-HSCT, but also improving the outcome of allo-HSCT.

Leukemia (2011) 25, 41–47; doi:10.1038/leu.2010.228; published online 14 October 2010

Keywords: Philadelphia chromosome-positive acute lymphoblastic leukemia; imatinib; allogeneic hematopoietic stem cell transplantation

Introduction

The Philadelphia chromosome (Ph) presents in 20–25% of adult patients with acute lymphoblastic leukemia (ALL) and is an

extremely unfavorable prognostic factor. The outcome of patients with Ph-positive ALL (Ph+ALL) following conventional chemotherapy is dismal, showing <20% long-term survival.^{1–4} Although allogeneic hematopoietic stem cell transplantation (allo-HSCT) has offered a curative option in Ph+ALL,^{3–5} relatively high rates of relapse and non-relapse mortality (NRM) impair the treatment success even after allo-HSCT. The International Bone Marrow Transplant Registry reported a leukemia-free survival rate of 38% following human leukocyte antigen (HLA)-identical allo-HSCT for Ph+ALL patients transplanted in the first complete remission (CR).⁶ Previously, we and others reported that imatinib-based chemotherapy produced very high CR rate, thus allowing a high proportion of patients to prepare for allo-HSCT.^{7,8} However, because of the short observation period, the impact of imatinib-based therapy upon the survival outcomes after allo-HSCT remains unclear. To address whether allo-HSCT after imatinib-based therapy is a superior treatment approach to that after conventional chemotherapy, we conducted a retrospective analysis of Ph+ALL patients who underwent allo-HSCT before and after imatinib became available, using data from the Japan Adult Leukemia Study Group (JALSG) Ph+ALL202 study and from the nationwide database of the Japan Society of Hematopoietic Stem-cell Transplantation (JSHCT) and the Japan Marrow Donor Program (JMDP).

Patients and methods

Data source and patient selection criteria

We compared the transplantation outcome of patients treated by the JALSG Ph+ALL 202 study (imatinib cohort) with those in the historical control data in the pre-imatinib era from the JSHCT and JMDP (pre-imatinib cohort), in which information on patient survival, disease status and long-term complications, including chronic graft-versus-host disease (cGVHD) and second malignancies, is renewed annually using follow-up forms.^{9,10} To

Correspondence: Associate Professor S Mizuta, Department of Hematology, Fujita Health University Hospital, 1-98 Dengakugakubo, Kutsukake-cho, Toyoake, Aichi 470-1192, Japan.

E-mail: mizuta@mb.ccnw.ne.jp

Received 23 June 2010; revised 15 August 2010; accepted 25 August 2010; published online 14 October 2010

attain an adequate level of comparability in terms of allo-HSCT, patients were selected according to the following criteria: (1) patients with *de novo* Ph+ALL; (2) age range of 15–65 years and (3) allo-HSCT during their first CR. A total of 122 patients who received allo-HSCT between January 1995 and December 2001 (before the approval of imatinib by the Japanese government) were selected. This study period of the pre-imatinib cohort included the pioneering period of cord blood transplantation (CBT) when the relevance of cell dose and HLA matching had not yet been recognized. Thus, the subjects were limited to those who received bone marrow (BM) or peripheral blood (PB) as a treatment graft.

Patients

Between September 2002 and May 2005, 100 newly diagnosed patients with Ph+ALL were registered to the JALSG Ph+ALL202 study, and received a phase 2 imatinib-combined chemotherapy as described previously.⁷ Ph+ALL was diagnosed by the presence of Ph through chromosome and/or FISH analysis, and positivity for *BCR-ABL* fusion transcripts detection by real-time quantitative polymerase chain reaction (RQ-PCR) analysis.

Of 97 patients who achieved CR, 60 patients received allo-HSCT in their first CR. Of these 60 patients, 9 patients who received unrelated CBT were excluded in this analysis because of the reason as described at the selection criteria for control patients in the pre-imatinib era. Thus, 51 patients transplanted between February 2003 and December 2005 were analyzed. In the JALSG Ph+ALL202 study, allo-HSCT was recommended after achieving CR if an HLA-identical donor was available. The stem cell source for allo-HSCT was chosen in the following order: (1) matched-related allo-HSCT; (2) HLA-A, B and DRB1 allele matched (6/6) or DRB1 one-allele mismatched-unrelated allo-BMT, if patients had no HLA-matched-related donor and (3) unrelated CBT or HLA-mismatched-related allo-HSCT, if they had no donors described in (1) and (2). A prophylaxis for GVHD was determined by each institute, but did not include T-cell depletion. The study was approved by the institutional review board of each participating center and conducted in accordance with the Declaration of Helsinki.

Definition of engraftment and GVHD

Engraftment day was defined as the first day of three consecutive days when the absolute neutrophil count was $\geq 0.5 \times 10^9/l$. Graft failure was defined as the lack of any sign of neutrophil recovery. Engraftment that occurred after day 60 was also considered to be a graft failure. Patients who died early (<day 29) were excluded from the analysis of engraftment. Acute GVHD (aGVHD) and chronic GVHD (cGVHD) were defined according to previously described standard criteria.¹¹

Quantitation of *BCR-ABL* transcripts

The copy number of *BCR-ABL* transcripts in BM was determined at a central laboratory using the RQ-PCR as described previously.⁷ To minimize the variability in the results because of differences in the efficiency of cDNA synthesis and RNA integrity among the patient samples, the copy number of the *BCR-ABL* transcripts was converted to molecules per microgram RNA after being normalized by means of *GAPDH*. The normalized values of the *BCR-ABL* copies in each sample were reported as *BCR-ABL* number of copies. At least 5.7×10^5 copies/ μ g RNA *GAPDH* levels were required in a sample to

consider a negative PCR result valid; otherwise, the sample was not useful for minimal residual studies. The threshold for quantification was 50 copies/ μ g RNA. The levels below this threshold were designated as 'not detected' or '<50 copies/ μ g'. In this study, the former was categorized as PCR negativity.

Minimal residual disease (MRD) at the time of HSCT was evaluated by the result of RQ-PCR within 30 days prior to transplantation.

Statistical considerations

The primary end point of this study was overall survival (OS) after allo-HSCT. Secondary end points included disease-free survival (DFS) and the incidence of aGVHD, cGVHD, NRM and relapse. We defined DFS events as relapse or death, whichever occurred earlier. The observation periods for OS were calculated from the date of transplantation until the date of the event or last known date of follow-up. The probabilities of OS and DFS were estimated using the Kaplan-Meier product limit method. The cumulative incidences of NRM, relapse, aGVHD and cGVHD were estimated as described elsewhere, taking the competing risk into account.¹² In each estimation of the cumulative incidence of an event, death without an event was defined as a competing risk. Risk factors for OS and DFS were evaluated by a combination of uni- and multivariate analyses. The following variables were evaluated for each analysis: imatinib-based therapy prior to HSCT, age group (under 40 versus 40 to 54 versus 55 and older), stem cell source (BM versus PB), HLA disparity (matched (HLA-identical siblings or 6/6 allele matched unrelated) versus mismatched), duration from diagnosis to HSCT and cGVHD as time-varying covariate (yes versus no). Univariate analysis was performed using Cox regression models or log-rank test. Multivariate analysis was performed using Cox proportional hazards regression model or competing risk regression model¹³ as appropriate. For the evaluation of time-varying events, such as aGVHD or cGVHD, upon clinical outcomes, we treated these as time-varying covariates. Differences among groups in terms of demographic characteristics were tested using the χ^2 or Mann-Whitney tests as appropriate. All statistical analyses were conducted using STATA 11 (STATA Corp., College Station, TX, USA).

Results

Patient characteristics

In the imatinib cohort, there were 29 males and 22 females, with a median age of 38 years (range, 15–64 years). Regarding transcript types, 36 patients had minor *BCR-ABL* and 15 had major *BCR-ABL*. In 5 patients, pre-treatment cytogenetic data were not available, and of the remaining 46 patients, 8 showed t(9;22) only, 36 had additional chromosome aberrations and 2 showed normal karyotype. Of 48 patients who were evaluable for MRD analysis, 36 patients achieved PCR negativity at the time of HSCT.

Some of the clinical and biological features (such as presence of additional chromosome aberrations, *BCR-ABL* subtype, MRD status at HSCT and performance status at HSCT) were not available in the pre-imatinib cohort and not included in the present analysis.

Table 1 lists the characteristics of patients included in this comparative analysis. Some of the clinical features were significantly different between two cohorts: age distribution at HSCT ($P=0.048$), conditioning regimens ($P<0.001$), GVHD prophylaxis ($P<0.001$) and duration from diagnosis to HSCT ($P=0.041$). The majority of patients received the preparatory